# Trace gas emissions from combustion of peat, crop residue, domestic biofuels, grasses, and other fuels: Configuration and FTIR component of the fourth Fire Lab at Missoula Experiment (FLAME-4)

**C. E. Stockwell[1], R. J. Yokelson[1], S. M. Kreidenweis[2], A. L. Robinson[3], P. J. DeMott[2], R. C. Sullivan[3], J. Reardon[4], K. C. Ryan[4], D. W. T. Griffith[5], L. Stevens[6]**

[1] University of Montana, Department of Chemistry, Missoula, MT, USA

[2] Department of Atmospheric Science, Colorado State University, Fort Collins, CO, USA

[3] Center for Atmospheric Particle Studies, Carnegie Mellon University, Pittsburgh, PA, USA

[4] USDA Forest Service, Rocky Mountain Research Station, Fire Sciences Laboratory, Missoula, MT, USA

[5] University of Wollongong, Department of Chemistry, Wollongong, New South Wales, Australia

[6] Unit for Environmental Sciences and Management, North-West University, Potchefstroom, South Africa

Correspondence to: R. J. Yokelson (bob.yokelson@umontana.edu)

**Abstract**

During the Fourth Fire Lab at Missoula Experiment (FLAME-4, October-November 2012) a large variety of regionally and globally significant biomass fuels was burned at the US Forest Service Fire Sciences Laboratory in Missoula, Montana. The particle emissions were characterized by an extensive suite of instrumentation that measured aerosol chemistry, size distribution, optical properties, and cloud-nucleating properties. The trace gas measurements included high resolution mass spectrometry, one- and two-dimensional gas chromatography, and open-path Fourier transform infrared (OP-FTIR) spectroscopy. This paper summarizes the overall experimental design for FLAME-4 including the fuel properties, the nature of the burn simulations, the instrumentation employed, and then focuses on the OP-FTIR results. The OP-FTIR was used to measure the initial emissions of 20 trace gases: $CO_2$, CO, $CH_4$, $C_2H_2$, $C_2H_4$, $C_3H_6$, HCHO, HCOOH, $CH_3OH$, $CH_3COOH$, glycolaldehyde, furan, $H_2O$, NO, $NO_2$, HONO, $NH_3$, HCN, HCl, and $SO_2$. These species include most of the major trace gases emitted by biomass burning and for several of these compounds it is the first time their emissions are reported for important fuel types. The main fire types included: African grasses, Asian rice straw, cooking fires (open (3-stone), rocket, and gasifier stoves), Indonesian and extratropical peat, temperate and boreal coniferous canopy fuels, US crop residue, shredded tires, and trash. Comparisons of the OP-FTIR emission factors (EF) and emission ratios (ER) to field measurements of

biomass burning verify that the large body of FLAME-4 results can be used to enhance the understanding of global biomass burning and its representation in atmospheric chemistry models.

Crop residue fires are widespread globally and account for the most burned area in the US, but their emissions were previously poorly characterized. Extensive results are presented for burning rice and wheat straw: two major global crop residues. Burning alfalfa produced the highest average $NH_3$ EF observed in the study ($6.63 \pm 2.47$ g kg$^{-1}$) while sugar cane fires produced the highest EF for glycolaldehyde (6.92 g kg$^{-1}$) and other reactive oxygenated organic gases such as HCHO, HCOOH, and $CH_3COOH$. Due to the high sulfur and nitrogen content of tires they produced the highest average $SO_2$ emissions ($26.2 \pm 2.2$ g kg$^{-1}$) and high $NO_x$ and HONO emissions. High variability was observed for peat fire emissions, but they were consistently characterized by large EF for $NH_3$ ($1.82 \pm 0.60$ g kg$^{-1}$) and $CH_4$ ($10.8 \pm 5.6$ g kg$^{-1}$). The variability observed in peat fire emissions, the fact that only one peat fire had previously been subject to detailed emissions characterization, and the abundant emissions from tropical peatlands all impart high value to our detailed measurements of the emissions from burning three Indonesian peat samples. This study also provides the first EF for HONO and $NO_2$ for Indonesian peat fires. Open cooking fire emissions of HONO and HCN are reported for the first time and the first emissions data for HCN, NO, $NO_2$, HONO, glycolaldehyde, furan, and $SO_2$ are reported for "rocket" stoves; a common type of improved cookstove. The HCN/CO emission ratios for cooking fires ($1.72 \times 10^{-3} \pm 4.08 \times 10^{-4}$) and peat fires ($1.45 \times 10^{-2} \pm 5.47 \times 10^{-3}$) are well below or above the typical values for other types of biomass burning, respectively. This would affect the use of HCN/CO observations for source apportionment in some regions. Biomass burning EF for HCl are rare and are reported for the first time for burning African savanna grasses. High emissions of HCl were also produced by burning many crop residues and two grasses from coastal ecosystems. HCl could be the main chlorine-containing gas in very fresh smoke, but rapid partitioning to aerosol followed by slower outgassing probably occurs.

## 1 Introduction

Biomass burning (BB) is the largest source of primary, fine carbonaceous particles and the second largest source of total trace gases in the global atmosphere (Bond et al., 2004, 2013; Akagi et al., 2011). Although a naturally occurring process, humans familiarized fire for various purposes including land management, pest control, cooking, heating, lighting, disposal, hunting, and industrial use (Crutzen and Andreae, 1990). The ever-growing global population contributes to increases in these anthropogenic practices; the injection of BB gas- and particle-phase emissions into the atmosphere; and critical climatic, radiative, chemical, and ecological impacts on local to global scales.

The primary carbon-containing gases emitted from biomass burning in order of abundance are carbon dioxide ($CO_2$), carbon monoxide (CO), and methane ($CH_4$), which includes two major greenhouse gases. BB is the second largest source of gas-phase non-methane organic compounds (NMOC) in the global atmosphere (Yokelson et al., 2008) and they have significant impacts on smoke evolution: particularly rapid formation of secondary organic aerosol (SOA) and secondary gases such as photochemical ozone ($O_3$) (Alvarado and Prinn, 2009; Reid et al., 1998). Other significant gas-phase primary emissions including nitric oxide (NO), nitrogen dioxide ($NO_2$) (van der A et al.,

2008), and nitrous acid (HONO) play important roles in the oxidative state of the atmosphere by contributing to both sources and sinks of the hydroxyl radical (OH), a primary atmospheric oxidant (Thompson, 1992). Bottom-up modeling of the local to global atmosphere requires emissions inventories that incorporate measurements of the amount of a trace gas or aerosol species emitted per unit fuel consumption (emission factors, EF). Top-down modeling can use known EF to constrain total fuel consumption at various geographic scales. Constructing comprehensive inventories for models requires emissions data for a variety of important fuel (ecosystem) types including savanna; temperate, boreal, or tropical forest; crop residue; peat; garbage burning; biofuels (e.g. cooking, charcoal making), etc. (Akagi et al., 2011; Wiedinmyer et al., 2011; Randerson et al., 2005; van der Werf et al., 2010). The characterization of the smoke emissions that result from fires burning a wide range of globally significant fuels is essential to model the initial impact and evolution of the emissions and their influence on local to global atmospheric chemistry.

Many different approaches are useful for characterizing BB emissions and aging. Field studies based on airborne or ground-based platforms characterize fires burning in the complex, natural environment. Airborne platforms are ideal for representative sampling of most fires and smoke aging while ground-based sampling can characterize un-lofted smoke, which is important on some fires (Bertschi et al., 2003a, 2003b; Akagi et al., 2012, 2013, 2014; Yokelson et al., 2013a). A third alternative: burning biomass fuels in a laboratory has been a useful way to characterize BB smoke (Christian et al., 2003; Goode et al., 1999; Yokelson et al., 1996, 2008, 2013a; McMeeking et al., 2009; Levin et al., 2010; Petters et al., 2009). Benefits typically include better fuel characterization, the opportunity to sample all the smoke from a fire, and quantification of more species/properties due to a more extensive suite of instrumentation. With this in mind, from October to November of 2012, a team of more than 40 scientists carried out the Fourth Fire Lab at Missoula Experiment (FLAME-4), which characterized the initial trace gas and particle emissions (and their subsequent evolution) from a wide variety of globally significant fuels including: African savanna grasses; crop-residue; Indonesian, temperate, and boreal peat; temperate and boreal coniferous canopy fuels; traditional and advanced cooking stoves; shredded tires; and trash.

In FLAME-4, the overarching goal was to burn both historically under-sampled and well-studied fuels while adding new instrumentation and experimental methods to provide previously unavailable information on smoke composition, properties, and evolution. A critical objective was to acquire this new information under conditions where the lab results can be confidently used to better understand real-world fires. In this respect the open-path Fourier transform infrared (OP-FTIR) spectroscopy system was especially helpful since it provided new emissions data and also measured many of the major inorganic and organic gaseous products of both flaming and smoldering combustion that overlapped well with the suite of fire emissions measured in numerous field campaigns. Thus, in FLAME-4, advanced lab measurements were combined with a lab-field comparison to enhance our understanding of important aspects of biomass burning including: (1) the effect of fuel type and fuel chemistry on the initial emissions; (2) the distribution of the emitted carbon among pools of various volatility in fresh and aged smoke with special attention to the large pool of unidentified semi-volatile organic gases identified in previous work (Yokelson

et al., 2013a); and (3) the factors influencing the evolution of smoke's chemical, physical, and cloud-nucleating properties.

This paper provides a brief overview of the FLAME-4 experiment (configurations used, fuels burned, and instruments deployed) and then focuses on a detailed description of the trace gas measurements by OP-FTIR. We present the major findings by OP-FTIR and compare lab and field data to inform the use of emissions data from the OP-FTIR and the extensive suite of other instruments deployed during the FLAME-4 burns. The other emissions data and the smoke aging results will be reported in separate papers and later synthesized in an organic-carbon apportionment paper similar to Yokelson et al. (2013a).

## 2 Experimental details

### 2.1 US Forest Service Fire Sciences Laboratory and configurations of the burns

The US Forest Service Fire Sciences Laboratory (FSL) in Missoula, Montana has a large indoor combustion room described in greater detail elsewhere (Christian et al., 2003; Burling et al., 2010). The room is 12.5 m × 12.5 m × 22 m high with a 1.6 m diameter exhaust stack joined to a 3.6 m diameter inverted funnel opening ~2 m above a continuously weighed fuel bed. The room is pressurized with conditioned, outdoor air to generate a large flow that entrains the fire emissions and vents them through the stack. A sampling platform surrounding the stack stands 17 m above the fuel bed and this is where most of the instrumentation was stationed during the first configuration of the experiment (hereafter "stack" burns). Other instruments were located in adjacent rooms with sampling lines pulling from ports at the sampling platform height. Previous studies found that the temperature and mixing ratios are constant across the width of the stack at the platform height, confirming well-mixed emissions that can be monitored representatively by many different sample lines throughout the fire (Christian et al., 2004). The room temperature and relative humidity were documented for each burn.

A set of twin smog chambers was deployed by Carnegie Mellon University (CMU) on the combustion room floor to investigate smoke aging with a focus on atmospheric processes leading to $O_3$ and SOA formation. The chambers consisted of fluorinated ethylene propylene (FEP) Teflon bags with UV lights affixed to the walls to initiate photochemical aging (Hennigan et al., 2011). Fresh BB smoke was drawn from the platform height in heated passivated sampling lines and introduced into the chambers after dilution to typical ambient levels using Dekati injectors. The smoke was then monitored for up to 8 hours by a large suite of instruments to examine initial and photochemically processed gas and aerosol concentrations and composition. The monitoring instruments included those in the CMU mobile lab, which was deployed just outside the building. We used the OP-FTIR to measure the pre-dilution smoke that filled the chambers, but we did not monitor the subsequently-diluted chamber contents via FTIR.

Experiments were conducted using two primary laboratory configurations. In the first configuration, "stack" burn fires lasting ~2-30 min were situated on a fuel bed located directly below the combustion stack described above. Emissions traveled upward through the stack at a constant flow rate while the instruments sampled continuously at

the platform height. The smoke was well mixed and had aged approximately 5 s by the time it reached the sampling height. In the second configuration, referred to hereafter as "room" burns, much of the instrumentation was relocated to other rooms immediately adjacent to the combustion room and air samples were drawn from lines projecting well into the combustion room. The combustion room was sealed and the fuels burned for several minutes. Within ~15-20 minutes the fresh smoke was well-mixed throughout the entire combustion room and was monitored while being "stored" in low-light conditions for several hours. $O_3$ and peroxyacetyl nitrate (PAN) remained below the sub-ppbv detection limits of the OP-FTIR during this storage period. Smoke emissions from "room" burns were also diluted into the smog chambers shortly after they became well mixed for further perturbation and analysis. These "room" burns were conducted primarily to allow more time-consuming analyses of the optical and ice-nucleating properties of smoke, which will be described in greater detail elsewhere (Levin et al., 2014). Figure 1 shows temporal profiles for CO and $CO_2$ excess mixing ratios during each configuration of the experiment and during distinct fuel-specific burns.

### 2.2 Fuels overview

This section summarizes the significance and authenticity of the fuels burned in this study. Selected properties are presented in Table 1, which includes the sampling location and dry weight percentage of carbon, nitrogen, and ash measured using a commercial CHN analyzer. Fuel chlorine and/or sulfur content are shown for selected fuels (Midwest Microlab LLC; ALS Environmental). Fuel loadings varied by fuel but were chosen to simulate real-world values, typically in the range of 0.1-5 kg $m^{-2}$ (Akagi et al., 2011). Global estimates of biomass consumption for several major fuel types investigated here are shown in Table 4 of Akagi et al. (2011). The fuels were primarily ignited with electric resistively heated coils, but for cooking fires and occasionally other fires, a propane or butane torch was used and small amounts of alcohol were sometimes required.

#### 2.2.1 South African and US grasses

Fire is a natural disturbance factor and valuable ecological management tool in grasslands, which are widespread globally. During the dry season in southern Africa, savannas are burned for reasons ranging from agricultural maintenance to grazing control (Govender et al., 2006). The fires consume aboveground biomass consisting mainly of grass with some litter and woody debris. Savanna fire emissions (mainly in Africa) have been estimated to contribute up to 44% of the total global pyrogenic carbon emissions in some years (van der Werf et al., 2011). A smaller, but significant fraction of the total pyrogenic emissions is attributed to this source by Wiedinmyer et al. (2010).

Savanna fuels burned during FLAME-4 were collected from experimental burn plots in Kruger National Park (KNP) in South Africa, a savanna ecosystem heavily prone to fire that has been the location of a number of ground- and aircraft-based campaigns measuring BB emissions (Wooster et al., 2011; Sinha et al., 2003; Yokelson et al., 2003a). We obtained tall- and short- grass samples from KNP near previous research sites (Shea et al., 1996) towards the peak of the fire season in September 2012. The tall-grass site (Pretoriouskop sourveld) is at an elevation of 560-640 m with an annual precipitation of ~700 mm. The landscape is dominated by tall, coarse grasses densely dispersed in

clumps throughout the area with very little tree or leaf litter. The short-grass site (Skukuza sweetveld) is at a lower elevation (400-480 m) with less precipitation (~570 mm) and was covered by much shorter grasses but included a greater amount of leaf litter. In both cases our lab simulations did not include the minor leaf component due to import restrictions.

Other grass samples burned included wiregrass, sawgrass, and giant cutgrass, all of which are common prescribed fire fuels in the southeastern US (Knapp et al., 2009). Wiregrass is frequently a significant component of the forest understory while the other two grasses are the major fuel components in coastal wildlife refuges. Prescribed burning in coastal marshes of the southeastern US is done to improve habitat for waterfowl (Nyman and Chabreck, 1995). All our US grass samples were collected in South Carolina.

#### 2.2.2 Boreal, temperate, and tropical peat samples

Peat deposits are accumulated, partially decomposed vegetation that is highly susceptible to combustion when dry and burns predominately by "creeping" surface or underground smoldering that is difficult to detect from space (Reid et al., 2013). Peat fires are the largest contributor to annual greenhouse gas emissions in Indonesia (Parker and Blodgett, 2008) and an estimated 0.19 - 0.23 Gt of carbon was released to the atmosphere from peat combustion during the 1997 El Niño, which was equivalent to ~40% of the mean annual global fossil fuel emissions (Page et al., 2002). This had major regional effects on health (Marlier et al., 2013) and climate (van der Werf et al., 2010).

Indonesian peat was sampled from three sites of the fire-prone area of the Mega Rice Project (MRP); a project that drained peatlands in Kalimantan for conversion to rice production that was subsequently abandoned. The first site had little evidence of ground disturbance with no indication of past burning, while the other sites were in highly degraded peat forest with reports of prior burn and logging events. The samples were collected at a depth of 10-20 cm below the surface and were cut into 10 cm × 10 cm × 10 cm blocks. The samples were dried step-wise in a microwave oven to a burnable moisture content.

Peat and organic soil can be a major fuel component for boreal fires (Turetsky et al., 2011). Our boreal peat samples were sub-humid boreal peat from the Hudson Bay Lowlands of Canada where most fires are caused by lightning. We also burned temperate swamp land peat collected in coastal North Carolina, which is subject to accidental fires and occasional prescribed burning. One North Carolina sample was obtained from the site of the large Pains Bay Fire (http://www.inciweb.org/incident/2218/; Rappold et al., 2011) in Alligator National Wildlife Refuge and the other from Green Swamp Preserve near Wilmington, NC.

#### 2.2.3 Open (3-stone), rocket stove, and gasifier cooking fires

Domestic biofuel use is thought to be the second largest type of global biomass burning in a typical year (Akagi et al., 2011). Approximately 2.8 billion people worldwide burn solid fuels (primarily biomass) indoors for household cooking and heating (Smith et al., 2013) and the smoke emissions contribute to an estimated 2 million deaths annually and chronic illness (WHO, 2009). Mitigating cooking fire emissions could alleviate adverse health effects

and substantial climate impacts (Kirchstetter et al., 2004; Ramanathan and Carmichael, 2008; Andreae and Ramanathan, 2013).

In this study, an experienced field researcher (L'Orange et al., 2012a, 2012b) simulated "field" cooking with four cookstove types and for five different fuels starting with the cookstove, pot, and water all at ambient temperature. Traditional 3-stone cooking fires are the most widespread globally and are simply a pot positioned on three stones or bricks above a continuously fed fuel center. The Envirofit Rocket G-3300 stove is an example of a common approach to reducing fuel consumption per cooking task. The "rocket" type insulated combustion chamber mixes cool air entering the stove with the heated combustion air and optimizes heat transfer to the pot via a vertical chimney (Bryden et al., 2005; MacCarty et al., 2008). The Ezy stove uses minimal material in a "rocket" type design with a patented inner chamber to focus heat. The Philips HD4012 "gasifier" type stove improves combustion efficiency with forced-draft air delivered by an internal fan (Roth, 2011).

A recent EPA study focused on the fuel-efficiency of various cooking technology options (Jetter et al., 2012) and FLAME-4 purposely included some similar fuels (red oak) and devices (3-stone, Envirofit G-3300 rocket stove, Philips HD4012 gasifier) to connect that work with our more detailed emissions speciation. The Ezy stove we tested was not included in the EPA study. Overall, fuel types for our cooking fire experiments included red oak, Douglas fir, and okote wood cut into 2 cm × 2 cm × 35.5 cm sticks and millet stalks all at ~5-10 % moisture content. We also measured the emissions from Douglas fir chips burned in the G-3300 rocket stove and Philips HD4012 gasifier stove.

**2.2.4 Crop residue fires**

Sugarcane is an important crop in some US states (LA, FL, HI) and parts of other countries (Brazil, South Africa, Mexico, etc.). Burning sugar cane before harvesting facilitates harvesting and can also have major regional air quality impacts (Lara et al., 2005). Globally, a broad range of other crop residues are burned post-harvest; often "loose" in the field, or in piles when associated with manual harvesting in the developing world (McCarty et al., 2007; Akagi et al., 2011). The fires enable faster crop rotation with less risk of topsoil loss; reduce weeds, disease, and pests, and returns some nutrients to the soil, but they are not yet well characterized and have a large atmospheric influence (Streets et al., 2003; Yevich and Logan, 2003; Chang and Song, 2010; Lin et al., 2010; Oanh et al., 2010; Yokelson et al., 2011; Sinha et al., 2014). The practice of burning agricultural residues on site is seasonally and regionally dependent and in the US may be unregulated or require permits (Melvin, 2012). The emissions from crop residue (CR) fires are often underestimated because (1) in common with all biomass burning, many of the gases are unidentified or rarely measured and (2) some algorithms for measuring burned area or active fire detection from space may miss some of the small, short-lived burns characteristic of crop-residue fires. Published space-based estimates of the area burned in crop residue fires in the US range from 0.26 to 1.24 Mha $yr^{-1}$ (Randerson et al., 2012; McCarty et al., 2009). In contrast Melvin (2012) found that ~5 Mha of croplands were burned in the US in 2011 based on state records, which would indicate that these fires account for the most burned area in the US. Better

characterization of the emissions from these diverse fuels for various burn conditions will address issue (1) and improve current inventories and models.

We burned various crop materials, which account for much of the agricultural burning in the US (McCarty et al., 2007) including sugar cane, rice straw, wheat straw from both conventional and organic farms, hay, and alfalfa collected from LA, CA, WA and MD, and CO, respectively. The crop materials from CO were sampled from an organic farm near Fort Collins and were burned to investigate the potential effects of agricultural chemicals on emissions of Cl, N, P, or S containing species (Christian et al., 2010; Becker et al., 2012; Eckhardt et al., 2007). Since crop residue fires are globally significant, we also burned authentic samples of millet from Ghana and rice straw from Taiwan, China, and Malaysia.

#### 2.2.5 US shrubland and coniferous canopy fires

Temperate ecosystems in the US and Canada experience both natural wildfires and prescribed fires with the latter being ignited to maintain habitats, reduce wildfire impacts, and open land access (Biswell, 1989; Wade and Lunsford, 1989). The effects of both wild and prescribed fires on air quality can be significant on local and regional scales (Park et al., 2007; Burling et al., 2011), necessitating a greater understanding of the emissions from fires in ecosystems such as chaparral and coniferous forests.

In a previous laboratory fire study extensive efforts were taken to reproduce complete fuel complexes for US prescribed fires with some success (Yokelson et al., 2013a; Burling et al., 2010). In this study we included similar chaparral fuels, but concentrated on just a part of the fuel complex for fires in coniferous forest ecosystems (fresh canopy fuels). Green boughs from MT ponderosa pine and AK black spruce were burned primarily to further investigate previous smog chamber smoke aging results using the same fuels (Hennigan et al., 2011).

#### 2.2.6 Tire fires

As the number of vehicles produced grew 5.1% from 2011 to 2012, the estimated total number of vehicles in use globally surpassed a billion (OICA, 2013). Parallel with this growth, tire disposal is a significant environmental concern because they end up in land-fills (including all non-biodegradable components) or being burned and producing emissions that are unfavorable to humans and the environment.

According to the US Scrap Tire Management Summary 2005-2009, 1946 of the 4002 tonnes of scrap tires generated in 2005 were used for fuel (RMA, 2011). Tires are useful as a fuel/coal substitute since the sulfur and nitrogen content is comparable to coal, but they produce more heat energy per unit mass (USEPA, 1997). Although ~48% of US scrap tires are recycled as fuel annually, the remainder, plus tires amassed across decades, are disposed of by alternative means including illegal dumps and informal or accidental fires that are notorious for becoming unmanageable and long-lasting. Tire disposal is also a major concern in developing countries where they may be used as fuel for minimally-regulated enterprises such as brick-kilns (Christian et al., 2010). To better characterize

the emissions from tire fires, we burned shredded tires identical to those involved in a major dump fire near Iowa City, IA.

### 2.2.7 Trash fires

McCulloch et al. (1999) estimated that 1500 Tg of garbage was produced for a world population of 4.5 billion with significant portions disposed of by open burning or incineration. Scaling to the current global population estimate of 7.05 billion (UNFPA, 2012), 2500 Tg of garbage is produced annually and the impact of disposal on local and global scales remains under-evaluated due partly to the lack of small burn detection by satellite. During ACE-Asia Simoneit et al. (2004a, b) observed that phthalates and n-alkanes that they attributed to trash burning accounted for ~10% of ambient organic aerosol mass in the central-west Pacific. In the US alone, it is estimated that 12-40% of households in rural areas burn garbage in their backyards (USEPA, 2006) and the airborne emissions could play a critical role in chemical deposition onto crops and soils. Lemieux et al. (1998, 2000, 2003) simulated open burning of household waste and concluded that this is a large US source of carbonyl and polychlorinated dibenzo-p-dioxins and polychlorinated dibenzofuran. Previous work has already established that garbage burning is an important source of black carbon (BC), ozone precursors, hydrogen chloride, particulate chloride and a variety of toxins including dioxins, hence better evaluation of this source is crucial (Costner, 2005; Christian et al., 2010; Li et al., 2012; Lei et al., 2013).

We ignited two fires that burned mixed, common waste collected daily at the FSL and another fire to separately measure the emissions from burning plastic shopping bags. The fuels we ignited for the garbage burns were intended to represent common household refuse with the understanding that household waste is highly variable. The overall carbon fraction for waste samples was determined by a procedure described in detail elsewhere (Christian et al., 2010). Briefly, the mass of each trash component was used to weight the carbon content of each component to calculate overall carbon content (IPCC, 2006; USEPA, 2006) as shown in Supplement Table S1.

## 2.3 Open-path FTIR data collection

The OP-FTIR deployed in FLAME-4 was used to measure the emissions of a suite of trace gases and consisted of a Bruker Matrix-M IR Cube spectrometer with a mercury-cadmium-telluride (MCT) liquid nitrogen cooled detector interfaced to a thermally stable 1.6 m base open-path White cell. The optical path length was 58.0 m and infrared (IR) spectra were collected at a resolution of 0.67 $cm^{-1}$ covering the range 600-3400 $cm^{-1}$. During "stack" burns the OP-FTIR was positioned on the sampling platform so that the open path spanned the width of the stack, allowing the continuously rising emission stream to be directly measured. For "stack" burns, four interferograms were co-added to give single ppbv detection limits at a time resolution of 1.5 s with a duty cycle greater than 95%. Spectral collection began a few minutes before fire ignition and continued throughout the fire. During the "room" burns, the OP-FTIR was removed from the stack but remained on the sampling platform in the combustion room. For the slower changing concentrations in this portion of the experiment, we increased the sensitivity by co-adding 16 interferograms (time resolution to 6 s) with continuous collection starting a few minutes before ignition and

continuing until all the smoke was exhausted from the room. A pressure transducer and two temperature sensors were located beside the White cell optical path and their outputs were logged and used to calculate mixing ratios from the concentrations determined from the IR absorption signals for both experimental configurations.

Mixing ratios were determined for carbon dioxide ($CO_2$), carbon monoxide (CO), methane ($CH_4$), ethyne ($C_2H_2$), ethene ($C_2H_4$), propylene ($C_3H_6$), formaldehyde (HCHO), formic acid (HCOOH), methanol ($CH_3OH$), acetic acid ($CH_3COOH$), glycolaldehyde ($C_2H_4O_2$), furan ($C_4H_4O$), water ($H_2O$), nitric oxide (NO), nitrogen dioxide ($NO_2$), nitrous acid (HONO), ammonia ($NH_3$), hydrogen cyanide (HCN), hydrogen chloride (HCl), and sulfur dioxide ($SO_2$) by multi-component fits to selected sections of the IR transmission spectra with a synthetic calibration non-linear least-squares method (Griffith, 1996; Yokelson et al., 2007) applying both the HITRAN spectral database and reference spectra recorded at Pacific Northwest National Laboratory (PNNL) (Rothman et al., 2009; Sharpe et al., 2004; Johnson et al., 2006, 2010). The selected spectral windows and hence interfering species depend strongly on resolution, relative humidity, pathlength, and concentration of the smoke. The spectral regions and parameters are re-optimized for most applications with current ranges reported in the supplementary information (Table S2), though we caution against using our settings in other work. Although nitrous oxide ($N_2O$) is fitted as part of the CO and $CO_2$ analysis, it is not reported because any enhancements are too small to be resolved confidently at 0.67 $cm^{-1}$ resolution. Even with higher resolution OP-FTIR significant $N_2O$ enhancements were not observed in smoke confirming it is at most a minor product (Griffith et al., 1991).

OP-FTIR offers several important advantages in the study of complex mixtures such as BB smoke. Each species exhibits a unique pattern of multiple peaks imparting resistance to interference from other species and aiding in explicit identification. The technique has no storage artifacts, it allows flexible sampling volumes that target multiple molecules simultaneously in the same parcel of air, and it provides continuous high temporal resolution data (Burling et al., 2010; Yokelson et al., 1996). Several million fitted retrievals provided real-time data for all 157 burns. On occasion a few of the target compounds were not present in detectable quantities during the course of certain fires. The uncertainties in the individual mixing ratios vary by spectrum and molecule and are dominated by uncertainty in the reference spectra (1-5%) or the detection limit (0.5-15 ppb), whichever is larger. OP-FTIR retrieval validation employs two main approaches: (1) interfacing the same FTIR to a closed cell that is challenged with appropriate pure and mixed gas standards at a similar path (e.g. Akagi et al., 2013) and (2) comparison to other techniques (e.g. GC or MS) in well mixed smoke (Goode et al., 1999; Christian et al., 2004; Veres et al., 2010). Uncertainties in fire-integrated amounts vary by molecule and fire, but are usually near 5% given the ppm-level concentrations. Errors closer to 10% may occur for a few molecules such as HONO (Veres et al., 2010). Fire-to-fire variability, even for the same nominal fuel, is the dominant uncertainty (often ~40%) and is reported by fuel type and species throughout.

### 2.4 Overview of other instruments

A goal of the FLAME-4 study was to extensively characterize the gas and aerosol emissions, therefore, a comprehensive suite of instrumentation was deployed. Here we list the other instruments deployed during the

campaign for reference purposes, but the results will be presented elsewhere. Gas-phase emissions were measured by OP-FTIR, a proton-transfer-reaction time-of-flight mass spectrometer (PTR-TOF-MS), two whole air sampling (WAS) systems, cartridge sampling followed by gas chromatography mass spectrometry (GC-MS), cartridge sampling followed by two-dimensional gas chromatography time-of-flight mass spectrometry (2D-GC-TOF-MS), a total hydrocarbon analyzer (THC), criteria gas monitors, and a proton-transfer-reaction (quadrupole) mass spectrometer (PTR-QMS).

Particle-phase instruments were deployed to measure aerosol chemistry, size distribution, optical properties, and cloud-nucleating properties. Particle chemistry measurements included gravimetric filter sampling of particulate matter with aerodynamic diameter < 2.5 microns ($PM_{2.5}$) followed by elemental carbon (EC) and organic carbon (OC) analyses and GC-MS and ion chromatography (IC) of extracts; an aethalometer; a high resolution time-of-flight aerosol mass spectrometer (HR-TOF-AMS); laser ablation aerosol particle time-of-flight (LAAP-TOF) single-particle mass spectrometer; and a particle-into-liquid sampler micro-orifice uniform-deposit impactor (PILS/MOUDI) to collect samples for several types of electrospray MS analyses (Bateman et al., 2010). Particle mass was also measured by a tapered element oscillating microbalance (TEOM$^{TM}$ 1405-DF). Chemistry and structure at the microscopic level were probed by collecting grids for scanning electron microscope (SEM) and transmission electron microscope (TEM) analyses.

Optical properties were measured by several single particle soot photometers (SP2); a photoacoustic extinctiometer (PAX); several photo-acoustic aerosol absorption spectrometers (PAS), PASS-3d (ambient/denuded), PASS-UV, the NOAA PAS system; and a broadband cavity enhanced absorption spectrometer (BBCEAS) (Washenfelder et al., 2013).

Size distributions were measured by several scanning mobility particle sizers (SMPS) and a fast mobility particle sizer (FMPS). Cloud nucleating properties of the aerosol were measured by a cloud condensation nuclei counter (CCNC), a continuous-flow diffusion chamber (CFDC) measuring ice nuclei, and a hygroscopic tandem differential mobility analyzer (H-TDMA). Supplement Table S3 provides a brief description of individual instrument capabilities and results from these instruments are reported elsewhere (e.g. Liu et al., 2014; Saleh et al., 2014; Tkacik et al., 2014).

**2.5 Emission ratio and emission factor determination**

We calculated excess mixing ratios (denoted $\Delta X$ for each species "X") for all 20 gas-phase species measured using OP-FTIR by subtracting the relatively-small average background mixing ratio measured before each fire from all the mixing ratios observed during the burn. The molar emission ratio (ER) for each species "X" relative to CO ($\Delta X/\Delta CO$) is the ratio between the sum of the $\Delta X$ over the entire fire relative to the sum of the $\Delta CO$ over the entire fire. A comparison of the sums is valid because the large entrainment flow ensures a constant total flow, but very small adjustments to these fire-integrated sums were made so they would represent the actual amount of emissions generated given the small changes in the emissions density that resulted from small changes in absolute temperature

and pressure over the course of some burns. Molar ER to CO were calculated for all the species measured using OP-FTIR for all 157 burns. The emission ratios to CO were then used to derive emission factors (EF) in units of grams of species X emitted per kilogram of dry biomass burned calculated by the carbon mass-balance method (CMB), which assumes all of the burned carbon is volatilized and that all of the major carbon-containing species have been measured (Ward and Radke, 1993; Yokelson et al., 1996, 1999; Burling et al., 2010):

$$EF(X)\left(g\,kg^{-1}\right) = F_C \times 1000 \times \frac{MW_x}{MW_C} \times \frac{\frac{\Delta X}{\Delta CO}}{\sum_{j=1}^{n}\left(NC_j \times \frac{\Delta C_j}{\Delta CO}\right)} \quad (1)$$

Where $F_C$ is the measured carbon mass fraction of fuel (see Table 1); $MW_x$ is the molecular weight of species X; $MW_C$ is the molecular weight of carbon; $NC_j$ is the number of carbon atoms in species j; $\Delta$Cj or $\Delta$X referenced to $\Delta$CO are the fire-integrated molar emission ratios for the respective species. The denominator of the third term in Eq. (1) estimates total carbon and the species $CO_2$, CO, and $CH_4$, which are all quantified by OP-FTIR, usually comprise 98-99% of the total carbon emissions for most fire types. By ignoring the carbon emissions not measured by OP-FTIR, emission factor estimates are typically inflated by a factor of ~1-2% (Andreae and Merlet, 2001; Yokelson et al., 2013a). Because of EF dependence on assumed total carbon, slightly different EF will appear in papers describing other instruments (Stockwell et al., 2014; Hatch et al., 2014). However, these differences are only a few percent (except for peat fires where they are ~5%) and insignificant compared to other uncertainties in global BB.

Emissions from fires are highly variable due in part to the naturally changing combustion processes; chiefly flaming and smoldering, which depend on many factors such as fuel geometry and moisture and environmental variables (Bertschi et al., 2003b; Yokelson et al., 2011). To estimate the relative amount of smoldering and flaming combustion that occurred over the course of each fire, we calculated a fire summed density-corrected modified combustion efficiency (MCE) for the fire (Yokelson et al., 1996):

$$MCE = \frac{\Delta CO_2}{\Delta CO_2 + \Delta CO} = \frac{1}{\left(1 + \left(\frac{\Delta CO}{\Delta CO_2}\right)\right)} \quad (2)$$

Though flaming and smoldering combustion often occur simultaneously, a higher MCE value designates relatively more flaming combustion (more complete oxidation) and lower MCE designates more smoldering combustion. "Pure" flaming combustion has an MCE of ~0.99 while pure smoldering typically has an MCE of ~0.8 (usual range 0.75-0.84). Thus, for example, an MCE of ~0.9 represents roughly equal amounts of flaming and smoldering. MCE can also be calculated for any point, or group of points, of special interest during a fire or as a time series (Yokelson et al., 1996), but that information is not explicitly presented in this paper.

### 2.6 Measurement strategy

Most biomass burning emissions inventories rely mainly on the average (i.e. the mean) EF obtained at the average MCE observed in airborne source measurements, when available, since most of the smoke from most field fires is entrained in a convection column making airborne measurements the most representative (Andreae and Merlet, 2001; Akagi et al., 2011). For fires that may be dominated by poorly lofted emissions, such as peat fires or residual smoldering combustion (Bertschi et al., 2003b), a ground-based MCE could be most representative. Laboratory fire experiments can provide measurements not available from field experiments or significantly increase the amount of sampling for fire-types rarely sampled in the field, but it is important to assess the representativeness of lab fire emission factors. The assessment of lab-derived EF is not completely straight-forward because BB produces highly variable emissions since field fires burn in a complex and dynamic environment that probably cannot be fully characterized safely. Fortunately, one parameter that correlates strongly with EF, MCE, has been measured on most field fires. "Ideal" lab fire simulations would burn with a range of MCE similar to that observed in natural fires. This is sometimes achieved, but is sometimes elusive due to differences in fuel moisture, wind, scale, etc (Yokelson et al., 2013a). Thus, a second, more readily achieved goal is for the lab fires to burn with a range in MCE that is broad enough to determine the EF dependence on MCE and then use this relationship to predict EF at the field-average MCE (Christian et al., 2003). In addition, even if lab fires differ from field fires in fire-integrated MCE, the ER to CO for smoldering compounds and the ER to $CO_2$ for flaming compounds is useful (Akagi et al., 2011). Finally, in the simplest approach the average ratio of field EF to lab EF can be applied as a correction factor to adjust lab EF (Yokelson et al., 2008). This approach was also warranted for adjustments to fuel-specific lab EF reported in Yokelson et al. (2013) because the results had the lowest error of prediction. When lab EF are adjusted it is not expected for instance that the EF versus MCE relationship will be identical in the lab and field or always be highly correlated, but simply that the adjustment procedure will nudge the EF in the right direction. We can take the level of agreement between the lab-based predictions and the airborne-measured averages (for species measured in both environments) as the most realistic estimate of uncertainty in using lab equations for species not measured in the field.

## 3 Results and discussion

We start this section by noting differences between "stack" (n = 125) and "room" (n = 32) burns. Figure 2 shows temporal profiles for the excess mixing ratios of the 19 gas-phase compounds we report for a complete "stack" burn. Figure 3 shows the excess mixing ratios of several gas-phase species during a typical "room" burn and highlights differences in their temporal behavior. For all gases in the room burn, a rapid rise and peak in concentration following ignition occurs because the OP-FTIR remained at a height of 17 m as described in Sect. 2.3. Rapid vertical mixing and then anticipated slow exchange from the combustion room account for the fast and then gradual decline in concentration for non-sticky species as revealed by the stable gases (e.g. CO and $CH_4$) shown in Fig. 3. The stickier gases undergo the same mixing processes, but decay at faster rates as illustrated by $NH_3$, $CH_3COOH$, HCOOH, and glycolaldehyde (decaying increasingly fast in the order given). These fast decays introduced error into the preliminary emission ratios to CO that were used to calculate provisional fire-integrated emission factors for

each fire. We assessed which gases were affected by this artifact by plotting EF vs MCE for each species for all 157 fires. If the room burn EF fell significantly below the general trend we assumed it was due to losses on the lab walls or aerosol surfaces. Supplement Tables S4 and S5 list all the "stack" and "room" burn EF/ER for all species and the average EF/ER for each fuel type along with uncertainties. The fuel type average EF/ER in the tables for "non-sticky" species (namely: $CO_2$, CO, $CH_4$, $C_2H_2$, $C_2H_4$, $C_3H_6$, $C_4H_4O$, NO, $NO_2$, HONO, HCN, $CH_3OH$, HCHO) are based on all 157 fires. Since the "room" burn EF/ER values for stickier species (HCl, $NH_3$, glycolaldehyde, $CH_3COOH$, HCOOH, and $SO_2$) are expected to be lower limit estimates, the average fuel type EF/ER for these species was calculated excluding "room" burn data. Next, in the sections below we note significant features of the OP-FTIR emission measurements and compare the emissions from each fuel type to field data when possible.

### 3.1 Emissions from African and US grasses

We measured a range of emissions from 20 African savanna grass fires that includes the first EF for HCl (0.26 ± 0.06 g $kg^{-1}$) for this fuel type and additional gases rarely measured for savanna fires such as $SO_2$, HONO, and glycolaldehyde (Sinha et al., 2003; Ferek et al., 1998; Trentmann et al., 2005). We also burned 30 fires with US grasses: giant cutgrass (8), sawgrass (13), and wiregrass (9). Previously, Goode et al. (1999) reported OP-FTIR EF for 13 trace gases from three laboratory fires burning western US bunchgrasses. Thus, our OP-FTIR data and the other anticipated results from FLAME-4 represent a large increase in emissions data for a major fuel component of fires across the US.

We discuss the chlorine emissions from grass fires first. Comprehensive vegetation analyses compiled by Lobert et al. (1999) show that grasses have much higher chlorine content on average than other common vegetative fuels. Thus, grass fires would be expected to emit more chlorine per unit biomass burned. The most studied chlorine-containing compound emitted from BB is methyl chloride, which was considered the largest natural contributor to organic chlorine in the atmosphere in the global reactive chlorine emissions inventory with about 50% contributed by BB (RCEI, Keene et al., 1999). HCl (an inorganic compound) was the Cl-containing gas quantified by OP-FTIR in this study and BB emissions of HCl were not considered in the RCEI. HCl is a "sticky" gas (Johnson et al., 2003; Komazaki et al., 2002; Webster et al., 1994) that readily adheres to surfaces, therefore, open-path optical systems are ideal for measuring primary HCl smoke emissions. In addition, the EF(HCl) for each FLAME-4 fuel type are positively correlated with MCE and the HCl mixing ratios consistently "track" with $CO_2$, $SO_2$, and $NO_x$ as seen in Fig. 2. This confirms HCl is a flaming compound and since grasses burn primarily by flaming combustion, high HCl emissions would be expected from this fuel. Our lab-average $\Delta HCl/\Delta CO$ ratio for savanna fires (the main global type of grass fire) is ~17 times higher than the $\Delta CH_3Cl/\Delta CO$ reported for savanna fires in Lobert et al. (1999) and still ~5 times higher after adjusting to the field average MCE of savanna grasses (0.938, see below). This indirect comparison suggests that HCl could be a major Cl-containing gas emitted by BB and the emissions could be significant. However, the gas-phase HCl mixing ratios decayed rapidly during our room burn storage periods and Christian et al. (2010) observed high particulate chloride with HCl below detection limits in the fresh emissions from Mexican crop residue fires. At longer time scales, particulate chloride has been observed to decrease as smoke ages (Li et al., 2003; Pratt et al., 2011; Akagi et al., 2012). Thus, both the rate at which HCl is initially incorporated

into the aerosol phase and the possibility that it is slowly reformed in aging plumes via outgassing of chlorine from particles remain to be investigated in detail.

Chlorine emissions from BB can also be affected by deposition of sea-salt, which can increase the Cl concentration of coastal vegetation (McKenzie et al., 1996). The highest average EF(HCl) for a fuel type during the FLAME-4 study was for sawgrass ($1.72 \pm 0.34$ g $kg^{-1}$). Both, the sawgrass and giant cutgrass were collected in a coastal wildlife refuge that is much closer to the Atlantic coast (~10 km) than the wiregrass sampling location (~165 km). The Cl-content listed in Table 1 and the measured EF(HCl) are consistent with the distance from the coast for the US grasses. The African grass EF(HCl) and Cl-content were lower than we measured for the coastal US grasses, but higher than the wiregrass values despite being collected further (225 km) from the coast, confirming that other factors besides distance from the coast effect grass Cl-content.

It is important to compare our FLAME-4 emissions data for African grass fires to field and other laboratory measurements of emissions from African savanna fires. Fig. 4 shows our EF results with those reported for similar African fuels burned at the FSL during February-March 2001 (Christian el al., 2003), airborne measurements from the SAFARI 2000 campaign (Yokelson et al., 2003a), and ground-based measurements from prescribed savanna fires in KNP (Wooster et al., 2011). We plot EF for smoldering compounds detected by all three sampling platforms versus MCE, providing an idea of the natural gradient in EF that result from savanna fuels and the impact measurement approach has on the type of combustion surveyed. The ground-based (long open-path FTIR), airborne (closed-cell FTIR) and laboratory based (open-path FTIR) emission factors can be fit to a single trend. The airborne average EF($NH_3$) is within the range of the ground-based EF($NH_3$) at the airborne average MCE, but at the low end likely due partly to natural variation in fuel nitrogen and partly because the correction for losses in the closed cell in the airborne system was not fully developed until later (Yokelson et al., 2003b). Both field studies observed much lower average MCE than both laboratory studies (likely due to higher fuel moisture, wind, smoldering roots, etc.), but the MCE is shown to correlate with much of the variation in EF.

Next, we exploit the MCE plot-based lab-field EF comparison as described in Sect. 2.6 to generate EF from our lab data that are more consistent with field studies. We plot lab and field EF versus MCE together for African savanna grasses in Fig. 5 with separate linear fits for comparison. The linear fit from the plot of lab EF versus MCE for each species is used to calculate an EF at the average MCE (0.938) from airborne sampling of authentic African savanna fires reported in Yokelson et al. (2003a). As shown in Table 2, this approach yields lab predicted EF that are, on average, only 21% different from field values and have even better agreement for hydrocarbon species (±3% including $CH_4$, $C_2H_2$, and $C_2H_4$). The lab-field comparison for nitrogen (N)-containing species has a higher coefficient of variation. Part of the larger variability could be the dependence of N-compound emissions on fuel nitrogen content in addition to MCE (Burling et al., 2010; McMeeking et al., 2009). Better lab-field agreement was obtained in an earlier application (Christian et al., 2003) of this approach for several compounds such as $CH_3COOH$, but that study featured a broader range of lab MCE that better constrained the fits. However, processing the data by this method improves the representativeness of the FLAME-4 EF across the board.

As an alternative to the plot-based analysis, despite the higher MCE of our lab fires, the ER for smoldering species to CO usually overlap with the field data at the one standard deviation level (Table 2, columns 5-7). This is important since most of the compounds emitted by fires are produced during smoldering and the lab ER (Table S5) can be considered reasonably representative of authentic savanna fires if used this way directly. Some species with "below-average agreement" using the EF approach do agree well using the ER approach and vice versa. Thus, neither approach is clearly preferred and both are adequate.

A comparison of our EF for US grasses with field work is not possible due to the lack of the latter type of measurements. However, it is likely that grass fires in the US burn with an average MCE that is lower than our lab average value of 0.961. This should have minimal impact on most of the ER to CO as discussed above; however, the lab EF versus MCE equations for US grasses could be used to calculate EF for US grasses at the African savanna field MCE (0.938) as shown in the final column of Table 2.

### 3.2 Emissions from Indonesian, Canadian, and North Carolina peat

FLAME-4 OP-FTIR data include the first emissions data for HONO and $NO_2$ for Indonesian peat fires (Table 3). The smoke measurements on three peat samples from Kalimantan represent a significant increase in information given the one previous study of a single laboratory burned sample from Sumatra (Christian et al., 2003). We also report EF from 4 fires burning extratropical peat that, along with other anticipated FLAME-4 results, adds significantly to the previous laboratory measurements of trace gases emitted by smoldering peat samples that were collected in Alaska and Minnesota (Yokelson et al., 1997). To our knowledge, all detailed chemical characterization of peat fire smoke has been done in the lab.

We discuss/compare the data now available for peat fire emissions from tropical and extratropical ecosystems. The average MCE of our Kalimantan peat fires (0.816) is comparable to the MCE reported for the Sumatran peat (0.838) burned previously by Christian et al. (2003). Figure 6 shows the ratio of our Indonesian peat EF as compiled in the supplementary information (Table S4) to those of Christian et al. (2003) for species reported in both studies displaying the range of our emissions as well as the study average. The greatest variation within the Indonesian peat fuels was that the single Sumatran peat fire emitted ~14 times more $NH_3$ per unit biomass combusted than the average of the "stack" burn Kalimantan samples, even though their MCE and percent nitrogen content were comparable (2.12% for Sumatran peat versus 2.27% for the Kalimantan peat). Comparing extratropical peat between studies, we find that 4.3 times larger $NH_3$ emission factors were observed for the peat burned by Yokelson et al. (1997) than from our FLAME-4 North Carolina and Canadian stack peat burns. For the extratropical case, only part of the higher levels seen earlier may be due to N-content differences (0.63-1.28% in FLAME-4 versus 0.78-3.06 % in Yokelson et al. (1997)). We suspect that part of the differences for $NH_3$ and other species seen in Fig. 6 (and discussed below) may be due to subtle, compound-specific fuel chemistry differences associated with the fact that the FLAME-4 samples evolved chemically at (and were collected at) greater depths than the samples burned earlier. Mineral content could vary (Table 1) and different logging/land-use histories could affect the incorporation of woody material. Another possible cause involves the drying method. In the previous studies the peat was allowed to

air dry to a very low moisture content (~5%) before ignition, whereas the FLAME-4 samples were stored wet and cool and then microwaved lightly just before ignition due to new United States Department of Agriculture (USDA) handling/storage restrictions. Drier peat may be consumed relatively more by glowing combustion, which could promote higher $NH_3$ and $CH_4$ emissions (Yokelson et al., 1997, Fig. 3).

The emissions also differed between the FLAME-4 Kalimantan peat and the earlier Sumatran peat study for N-containing gases that we measured other than $NH_3$ as shown in Fig. 7, namely HCN and $NO_x$. The FLAME-4 Kalimantan peat fire $NO_x$ emissions are 4.2 times higher than previously reported for Sumatran peat, which could impact the predictions of chemical transport models since $NO_x$ emissions strongly influence $O_3$ and SOA production in aging BB plumes (Trentmann et al., 2005; Alvarado and Prinn, 2009; Grieshop et al., 2009). Larger emissions of $NO_x$ from the Kalimantan peat samples likely occurred because two of the Kalimantan peat samples briefly supported spontaneous surface flaming whereas the Sumatran peat sample was completely burned by smoldering combustion and $NO_x$ is primarily produced during flaming combustion. The large range in EF(HCN) observed (1.38 – 7.76 g $kg^{-1}$) when considering all peat-burning studies adds uncertainty to any use of this compound as a tracer for peat fires (Akagi et al., 2011). Although there are noticeable differences between the Kalimantan and Sumatran laboratory fires, with this study we have quadrupled the amount of data available on Indonesian peat, which likely means the new overall averages presented in Table 3 are closer to the regional averages than the limited earlier data despite the high variability.

Sulfur emissions are also variable between peat fire studies. The lack of observed $SO_2$ emissions from our Kalimantan peat fires is noteworthy since earlier studies of Kalimantan smoke attributed heterogeneous aerosol growth to $SO_2$ emitted from peat fires with support by unpublished laboratory data (Gras et al., 1999). We did detect small amounts of $SO_2$ from one of three NC peat fires, but, despite a careful search, no OCS was detected, which was the only sulfur containing compound detected in previous extratropical peat fire studies (Yokelson et al., 1997).

The emissions of $CH_4$ from biomass fires make a significant contribution to the global levels of this greenhouse gas (Simpson et al., 2006). The EF($CH_4$) measured for BB studies in general exhibit high variability with higher emissions at lower MCE (Burling et al., 2010). We observed high variability in EF($CH_4$) at similar MCEs for our Kalimantan peat samples (range 5.72 - 18.83 $kg^{-1}$) with our upper end comparable to the EF($CH_4$) previously reported for the Sumatran peat sample (20.8 g $kg^{-1}$). Sumatran peat may burn with high variability, but with only one sample there is no probe of this. Emission factors for $CH_4$ from extratropical peat are also consistently high (4.7 - 15.2 g $kg^{-1}$). Taken together, all the FLAME-4 results, earlier measurements of EF($CH_4$) for peat, and field measurements of fuel consumption by peat fires (Page et al., 2002; Ballhorn et al., 2009) suggest that peat fires are a significant source of $CH_4$, an important infrared absorber in our atmosphere (Forster et al., 2007; Worden et al., 2013).

### 3.3 Cooking fire emissions

Biofuel combustion efficiency and emissions depend on the stove design, type and size of fuel, moisture, energy content, and each individual's cooking management (e.g. lighting and feeding) (Roden et al., 2008). The fire-

575 averaged emissions of species we measured by OP-FTIR for four types of stoves and five fuel types are reported in
576 Table 4. From the OP-FTIR data alone we report the first EF for HCN for open cooking fires; the first EF for HCN,
577 NO, $NO_2$, HONO, glycolaldehyde, furan, and $SO_2$ for rocket stoves; and the first large suite of compounds for
578 gasifier devices.

579 We begin with a brief discussion of the first HCN measurements for cooking fires. HCN is emitted primarily by
580 biomass burning (Li et al., 2000) and can be used to estimate the contribution of BB in mixed regional pollution,
581 most commonly via HCN/CO ratios (Yokelson et al., 2007; Crounse et al., 2009). HCN was below the detection
582 limit in previous cooking fire studies using an FTIR system with a short (11 m) pathlength leading to speculation
583 that the HCN/CO emission ratio was low for commonly used wood cooking fuels (Akagi et al., 2011). In FLAME-4,
584 the higher sensitivity FTIR and longer pathlength allowed FTIR detection of HCN on a few cooking fires and the
585 HCN/CO emission ratio ($1.72 \times 10^{-3} \pm 4.08 \times 10^{-4}$) is about a factor of 5 lower than most other BB fuels burned in
586 this study; excluding peat, which had anomalously high HCN/CO ratios up to ($2.26 \times 10^{-2}$). The divergent HCN/CO
587 ratios for these two types of BB should be considered when using HCN to probe pollution sources in areas where
588 one or both types of burning are important (e.g. Mexico, Indonesia).

589 Since minimizing cooking fire fuel consumption is a paramount concern for global health, air quality, and climate, it
590 is of great interest to compare the FLAME-4 cooking fire results, which are of unprecedented detail, to a major
591 cookstove performance study by Jetter et al. (2012). We assess the validity of synthesizing results from these two
592 important studies using the handful of gases measured in both studies ($CO_2$, CO, and $CH_4$). In Fig. 8 we have
593 averaged emissions for all fuels for these three species by stove type for the traditional 3-stone fires, the Envirofit
594 rocket stove, and the Philips gasifier stove and compared to identical stoves burning red oak fuel in the performance
595 testing reported by Jetter et al. (2012). We show the ratio of our fire-average (ambient start) EF to the EF reported
596 by Jetter et al. (2012) specific to different operating conditions in their tests: i.e. when the cookstove had (1) an
597 ambient temperature start, (2) hot-start, and (3) when water in the cooking pot started from a simmer. The FLAME-4
598 emissions of $CO_2$, CO, and $CH_4$ for the traditional 3-stone and Envirofit rocket designs agree very well with the
599 performance-oriented emissions data for ambient- and hot- start conditions. We obtained higher emissions than
600 Jetter et al. (2012) for the Philips gasifier type stove, but the 3-stone and rocket designs are much more widely-used
601 than the gasifier globally and, in general, lower performance may have more relevance to real world use (see below).
602 In any case, the comprehensive emissions speciation in FLAME-4 can be combined with the performance testing by
603 Jetter et al. (2012) to better understand the major currently-used global cooking options with reasonable confidence.
604 We note that our focus was comprehensive emissions speciation, but point out that our traditional 3-stone fires took
605 the longest time to reach a steady state, consumed the most fuel, and produced higher mixing ratios of pollutants for
606 their respective fuel types as shown in Fig. 9.

607 We now compare our FLAME-4 OP-FTIR-based open cooking fire EF to field measurements of the EF from 3-
608 stone cooking fires for the few trace gases measured fairly widely in the field (essentially $CO_2$, CO, and $CH_4$).
609 Figure 10 shows study-average EF($CH_4$) versus MCE for a number of studies including: field data from Zambia
610 (Bertschi et al., 2003a), Mexico (Johnson et al., 2008; Christian et al., 2010), and China (Zhang et al., 2000);

611 laboratory data from FLAME-4 and Jetter et al. (2012); and recommended global averages (Andreae and Merlet
612 2001; Akagi et al., 2011; Yevich and Logan, 2003). The range of MCE demonstrates the natural variability of
613 cooking fire combustion conditions. We observe a strong negative correlation of EF($CH_4$) with MCE ($R^2$ = 0.87)
614 that includes all the studies. However, the Jetter et al. (2012) study and especially FLAME-4 are offset to higher
615 MCE than the field average. As discussed earlier, this may reflect more efficient stove use sometimes observed in
616 lab studies. More representative lab EF can readily be calculated from the MCE plot-based comparison (described in
617 Sect. 2.6). The FLAME-4 EF agree well with the field data after adjustment by this approach and we use it to project
618 EF for species not measured in the field: namely HCN (0.071 g $kg^{-1}$) and HONO (0.170 g $kg^{-1}$), which we report for
619 the first time, to our knowledge, for open cooking. The $\Delta HONO/\Delta NO_x$ is ~13% confirming that HONO is an
620 important part of the cooking fire $NO_x$ budget. As noted above for other BB types, the lab ER of smoldering
621 compounds to CO are also fairly representative and included for open cooking in Table 4.

622 We also compare with the limited field measurements of rocket stove emissions. The FLAME-4 EF of species
623 available for comparison generally agree within one standard deviation of the Christian et al. (2010) field Patsari
624 cookstove data. Thus, despite the small sample size, we conclude that the FLAME-4 ER, EF, and measurements to
625 be presented elsewhere (such as aerosol optical properties) for these advanced cookstoves can likely be used directly
626 with some confidence to assess the atmospheric impact of using these stoves.

627 **3.4 Emissions from crop residue fires**

628 FLAME-4 provides the first comprehensive emissions data for burning US crop residue and greatly expands the
629 emissions characterization for global agricultural fires. The EF and ER for all the crop residue (CR) fuels burned
630 during FLAME-4 are compiled in Tables S4 and S5 in the Supplement. Upon initial assessment of these data, a
631 distinction between two groups emerges. To illustrate this, the EF dependence on MCE for $NH_3$ emitted by burning
632 CR fuels is illustrated in Fig. 11. The EF($NH_3$) from alfalfa and organic hay are much larger than for the other crops
633 at all MCE, which makes sense as these crops are high in N (Table 1) and are grown partly to meet the high protein
634 needs of large livestock. The EF($NH_3$) for millet was smaller than for the other CR fuels. The millet EF could differ
635 because of inherent low N content (Table 1) or possible N losses since the samples were collected a year prior to
636 burning. Alfalfa, hay, and millet were also outliers in the EF versus MCE plots made for other trace gases. The
637 remaining fuels, sugar cane and especially rice straw and wheat straw are associated with important crops grown for
638 human nutrition and these three were grouped together to compare laboratory CR fire emissions to the limited
639 available field data as detailed later.

640 Crops are domesticated "grasses" that would be expected to have high Cl content. The use of agricultural chemicals
641 could further increase Cl content and/or Cl emissions. HCl is the Cl-containing species we could measure with OP-
642 FTIR and its emissions are correlated with flaming combustion as noted earlier. The highest CR EF(HCl) (0.923 g
643 $kg^{-1}$) was observed for the CR (Maryland wheat straw) with the highest Cl content (2.57%). As seen in Table 1, the
644 Cl content of the two conventional wheat straw samples varied significantly with the sample from the east shore of
645 MD being much higher than the inland sample from WA. However, even though the organic wheat straw from

Colorado had much lower Cl content than the conventional wheat straw from MD it was significantly higher in Cl than the conventional wheat straw from WA that was also sampled closer to the coast. This confirms our earlier statement that Cl content can depend on more than the distance from the coast for similar vegetation. In addition, the high variability in Cl indicates that measuring the extent to which agricultural chemicals may contribute to vegetation Cl content and/or Cl emissions would require a more precise experiment where only the applied chemical regime varies. Nevertheless, we confirm above average initial emissions of HCl for this fuel type.

Other notable features of the CR fire emissions are discussed next. Of all our FLAME-4 fuels, sugarcane fires had the highest average EF for formaldehyde, glycolaldehyde, acetic acid, and formic acid. Glycolaldehyde is considered the simplest "sugar-like" molecule; it has been reported as a direct BB emission in laboratory-, ground-, and aircraft-based measurements by FTIR and its atmospheric chemistry (including as an isoprene oxidation product) has been discussed there-in (Yokelson et al., 1997; Akagi et al., 2013; Ortiz-Montalvo et al., 2012; Johnson et al., 2013). In Fig. 12, we show the EF(glycolaldehyde) as a function of MCE for our FLAME-4 CR fires, all remaining FLAME-4 fuels, a series of airborne measurements from US field campaigns (in 2009-2011) (Johnson et al., 2013), and older laboratory measurements of smoldering rice straw (Christian et al., 2003). The FLAME-4 CR fires have significantly higher EF than the pine-forest understory and shrubland fires discussed in Johnson et al. (2013), but rice straw fire measurements by Christian et al. (2003) adjusted to reflect the new PNNL reference spectrum have even higher EF for both glycolaldehyde and acetic acid in comparison to our current sugarcane measurements. The higher EF in the previous lab study are consistent with the lower MCE that resulted from burning the rice straw in dense piles similar to those observed in Indonesia where manual harvesting is common (Christian et al., 2003).

Next we compare the FLAME-4 CR fire EF to the limited field data available. Although CR fire emissions are undoubtedly affected by crop type and burning method (loosely packed and mostly flaming versus piled and mostly smoldering), this type of specificity has not been implemented in atmospheric models to our knowledge. All available ground-based and airborne field measurements of CR fire EF were averaged into a single set of EF for burning crop residue in the field by Akagi et al. (2011) in their supplementary Table 13. The average ratio of our FLAME-4, MCE plot-based EF predictions for 13 overlapping species to the field EF is close to one with the good agreement reflecting some cancellation of positive and negative offsets (Table 5). The lab and field ER are also shown to agree very well. The mostly small differences that do occur between the FLAME-4 lab-predicted EF and the field studies could be due to differences in fuel, burning conditions, and sampling regions. The field CR fire EF are all from Mexico (Yokelson et al., 2009, 2011; Christian et al., 2010) while FLAME-4 measured EF for a variety of fuels from Colorado, Washington, California, Louisiana, China, Taiwan, and Malaysia (see Sect. 2.2.4). Data from recent airborne campaigns sampling US CR fires including SEAC$^4$RS (Studies of Emissions, Atmospheric Composition, Clouds and Climate Coupling by Regional Surveys, www.nasa.gov/mission_pages/seac4rs/index.html) and BBOP (Biomass Burn Observation Project, www.bnl.gov/envsci/ARM/bbop) will provide valuable comparisons to our FLAME-4 CR fire EF at a later date.

### 3.5 Emissions from US shrubland and coniferous canopy fires

We burned fresh boughs from the following coniferous vegetation that is widespread in the western US and Canada: ponderosa pine, black spruce, and juniper. The canopy of these trees/shrubs is sometimes consumed in prescribed burns, but that is more commonly the case in wildfires, especially crown fires. However, these fuels were not burned to simulate real, complete wildfire fuel complexes: rather they were of interest as an extension of FLAME-3 smog chamber experiments investigating organic aerosol (OA) transformations (Hennigan et al., 2011). In FLAME-3 black spruce produced the most secondary organic aerosol (SOA) upon aging while ponderosa pine produced the least SOA. The SOA results for these and other fuels from FLAME-4 will be reported separately (Tkacik et al., 2014). The OP-FTIR data (Tables S4 and S5) is of value to characterize the starting conditions in the smog chambers. For instance, in FLAME-4 the ponderosa pine burns were characterized by a lower MCE (0.917 ± 0.032 , range 0.839-0.952), hence more smoldering-dominated burns than the black spruce burns (MCE 0.951 ± 0.012, range 0.933 - 0.970). Both ponderosa pine and spruce boughs were also burned in the lab fire study of Yokelson et al. (2013a) and, collectively with the FLAME-4 measurements, we now have more detailed information on the initial emissions from these fuels than was available during the FLAME-3 campaign.

There are just a few published field measurements of emissions from chaparral fires, which include: (1) Airborne measurements of EF reported by Burling et al. (2011) for 16 of the trace-gas species also measured in this work for five California chaparral fires and (2) a limited number of trace gases reported by Radke et al. (1991) and Hardy et al. (1996) for prescribed chaparral burns. For these published field studies as a group the average EF is 0.935 ± 0.011.We combined the seven chamise and three manzanita burns from FLAME-4 to represent chaparral fuels and obtained a slightly lower lab-average MCE of 0.929 ± 0.017 (spanning a range of 0.903-0.954, see Table S4). The lab MCE and EF agree well with the MCE and EF from field measurements, which suggests that FLAME-4 measurements can be used directly and confidently including for species and properties not yet measured in the field. The emissions data from recent field studies of wildfires (SEAC$^4$RS, BBOP) that burned some coniferous canopy and chaparral fuels can be compared with our FLAME-4 EF in the future.

**3.6 Emissions from tire fires**

To our knowledge, FLAME-4 presents the first comprehensive emissions data for burning tires. Emissions are affected by fuel composition and tires are composed of natural and synthetic rubber, carbon black, fabric, reinforcing textile cords, steel-wired fibers and a number of chemical accelerators and fillers added during the manufacturing process (Mastral et al., 2000). One such additive is sulfur which is essential during the vulcanization process in creating rigid and heat resistant tires. The sulfur could be emitted during combustion of tires in various forms including $SO_2$, which is a monitored, criteria air pollutant chiefly because atmospheric oxidation of $SO_2$ results in acid rain and sulfate aerosol particles that are a major climate forcing agent with adverse effects on human health (Schimel et al., 1996; Lehmann and Gay, 2011; Rohr and Wyzga, 2012 ). For the two tire burns conducted during FLAME-4 the average MCE was 0.963; burns dominated by flaming combustion. $SO_2$ is a product of flaming combustion (see Fig. 2 or Lobert et al., 1991) and our tire samples likely contained high amounts of S that was efficiently converted to $SO_2$ by the high MCE burns resulting in a very high average EF($SO_2$) of 26.2 ± 2.2 g kg$^{-1}$. To put this in perspective, our second largest EF($SO_2$) arose from giant cutgrass (3.2 g kg$^{-1}$), which was about

three times the typical FLAME-4 EF($SO_2$) of ~1 g $kg^{-1}$. About ~48% of the scrap tires generated in the US in 2005 (RMA, 2011) were used as fuel (coal substitute) and this was the fate of ~20% of the scrap tires in Canada in 2004 (Pehlken and Essadiqi, 2005). However, our calculations suggest that tire combustion only contributed ~0.5% of $SO_2$ emissions for the US and Canada in 2005 (Smith et al., 2011). Meanwhile, combustion of fossil fuels, specifically coal, was estimated to account for 56% of the world $SO_2$ emissions in 1990 (Smith et al., 2001). Despite the low total global significance compared to coal it is quite possible for the $SO_2$ and other combustion products from tire burning to have important local effects (http://thegazette.com/2012/06/01/how-is-iowa-city-landfill-fire-affecting-air-quality/).

Many species including HONO, $NO_2$, HCN, $CH_3COOH$, HCOOH, and furan were quantified for the first tire burn (~500 g) but fell below the detection limit during the second smaller fire (~50 g). For one such species, gas-phase nitrous acid (HONO), tire burning produced the largest EF (1.51 g $kg^{-1}$) of the entire study. Daytime photolysis of HONO serves to form NO and the atmospheric oxidant OH on a timescale of 10-20 min (Schiller et al., 2001). To normalize for differences in the nitrogen content of fuels shown in Table 1, it is useful to compare ΔHONO to $\Delta NO_x$. The ER($\Delta HONO/\Delta NO_x$) for tire burns (19%) is incidentally within the typical range of ~3-30% for BB studies compiled in Akagi et al. (2011). The EF of HONO (1.51g $kg^{-1}$) and $NO_x$ as NO (3.90 g $kg^{-1}$) were among the largest for this study while the EF(HCN) was small (0.36 g $kg^{-1}$) and $NH_3$ remained below the detection limit even in the bigger tire fire. These results suggest that much of the fuel nitrogen is converted to $NO_x$ and HONO and that the mid-range N-content estimated for tires by Martinez et al. (2013) shown in Table 1 (0.57%) is large enough to support the observed EF.

**3.7 Emissions from burning trash and plastic bags**

Published measurements of trash burning emissions are rare. The FLAME-4 measurements are the first to report EF for glycolaldehyde for trash burning. Since it is difficult to be confident about waste simulation, we first assess the relevance of the FLAME-4 trash fire simulations by comparison to the limited previous data. The emissions from burning simulated military waste were evaluated in two previous studies for a number of species not measured by OP-FTIR including polycyclic aromatic hydrocarbons, particulate matter, several volatile organic compounds (VOC), polychlorinated or brominated dibenzodioxins, and furans (Aurell et al., 2012; Woodall et al., 2012). These two studies are not discussed further here. In Supplement Table S6 we show the EF from the two trash burns in FLAME-4 and "overlapping" previously-published garbage burning EF including those from 72 spot field measurements of fires in authentic Mexican landfills reported by Christian et al. (2010), an airborne campaign that sampled a single dump fire in Mexico (Yokelson et al. 2011), and a single previous laboratory simulation (Yokelson et al., 2013a).

The first FLAME-4 trash fire simulation had much higher HCl, HCHO, and glycolaldehyde and lower $NO_x$, $NH_3$, and $SO_2$ than the second simulation. The average of the two FLAME-4 burns and most of the trash fire EF we measured in FLAME-4 are well within the range observed in the field for hydrocarbons and the oxygenated organic compounds except for acetic acid which had mixing ratios below the detection limit in FLAME-4. The increase in

753 estimated carbon content between studies accounts for the considerable increase in EF($CO_2$) for the FLAME-4
754 burns. The EF reported in Supplement Table S6 for field data assumed an overall carbon fraction of 40% while an
755 estimated value of ~50% was calculated for FLAME-4 waste. There were significantly lower emissions of N-
756 containing compounds and HCl in the FLAME-4 trash burn simulations compared to the Mexican landfill fires. The
757 single laboratory trash fire EF(HCl) reported by Yokelson et al. (2013a) (10.1 g $kg^{-1}$) and the higher of two EF(HCl)
758 from FLAME-4 (1.52 g $kg^{-1}$) lie close to the upper and lower end of the actual Mexican landfill fire results (1.65-9.8
759 g $kg^{-1}$). Based on the EF(HCl) of pure polyvinyl chloride (PVC) reported in Christian et al. (2010) we expected a
760 higher EF(HCl) correlated to the high PVC mass percentage (9.8%) in our simulated trash sample that contained
761 PVC. The EF(HCl) is affected by the combustion factor of the PVC itself and the actual percent burned may have
762 been low during our simulation. The differences between the emissions of Mexican landfill fires and our laboratory
763 garbage fires likely reflect the general difficulty of simulating real-world landfill content; in particular we likely
764 underrepresented a nitrogen source such as food waste in lab simulations. While a more realistic representation of
765 complex, real-world waste would have been ideal, the FLAME-4 data should be useful for enhancing our knowledge
766 of the emissions from some components of this globally important, but under-sampled source.

767 We burned one trash component separately in one fire: namely plastic shopping bags. Much of the plastic produced
768 globally ends up in landfills with alternative means of disposal including incineration, open burning, or use as an
769 alternative household fuel in developing countries. It has been estimated that 6.6 Tg $CO_2$ was generated from the
770 incineration of plastics in waste in 2011 in the US and that incineration is the disposal method for 7-19 percent of
771 waste in the US generating an estimated 12 Tg $CO_2$ annually (USEPA, 2013). Shopping bags primarily consist of
772 high and low density polyethylene (HDPE, LDPE) with a carbon content of 86%, the highest value in this study
773 (USEPA, 2010). The EF($CO_2$) of 3127 g $kg^{-1}$ is slightly larger than that from shredded tires (2882 g $kg^{-1}$). During the
774 single burn of "pure" plastic bags, flaming combustion dominated more than in any other FLAME-4 fire, as can be
775 seen in the high MCE (0.994), the steady high ratio of $\Delta CO_2/\Delta CO$ (Fig. 13) and by the fact that many smoldering
776 combustion species remained below the OP-FTIR detection limit. In this respect, plastic bags are higher quality fuel
777 than biomass although less-controlled combustion of mixed refuse, or a mix of plastics and biomass, would likely
778 result in less efficiency and greater EF for smoldering species.

779 **4 Conclusions**

780 We used open-path FTIR to measure the emissions of 20 of the most abundant trace gases produced by laboratory
781 burning of a suite of locally to globally significant biomass fuels including: African savanna and US grasses; crop-
782 residue; temperate, boreal, and Indonesian peat; traditional cooking fires and cooking fires in advanced stoves; US
783 coniferous and shrubland fuels; shredded tires; and trash. We report fire-integrated emission ratios (ER) to CO and
784 emission factors (EF, grams of compound emitted per kilogram of fuel burned) for each burn. The fire-type average
785 EF and ER for sticky species (HCl, $NH_3$, HCOOH, $CH_3COOH$, glycolaldehyde, $SO_2$) are computed without the data
786 from the room burns (due to losses on aerosol or lab surfaces) as indicated in Tables S4 and S5 in the Supplement.

Many of the fire-types simulated have large global significance, but were not sampled extensively in the past. The fire types simulated that have been subject to extensive past study were sampled with new instrumental techniques in FLAME-4. In either case it is necessary to establish the relevance of the lab simulations by comparison to field data when available. The emissions from field fires depend on a large number of fuel and environmental variables and are therefore highly variable. Laboratory biomass burning can sometimes occur with a different average ratio of flaming to smoldering combustion than is observed for field fires in similar fuels. Smoldering combustion produces the great majority of measured emitted species and we find that our ER to CO for smoldering compounds are normally similar to field results. Based on lab/field comparisons, we conclude that our lab-measured EF for some of the fires can be adjusted to better represent typical open burning. We describe a straight forward procedure for making these adjustments when warranted. For some fuels there is only lab emissions data available (e.g. peat and tires) and we must rely solely on that. In other cases (e.g. rocket stoves and chaparral) both the lab ER and EF can be used directly to supplement field data. For some fuels (e.g. African grasses and crop residue) the ER can be used directly and we provide a procedure to adjust the lab EF that is based on analysis of the overlap species and has a characterized uncertainty. Thus, all the FLAME-4 results for various species and properties, especially those yet unmeasured in field studies, should be useful to enhance the understanding of global biomass burning. As mentioned above, this is important in part because the smoke characterization in FLAME-4 featured the first use of many instruments, the first sampling with some instruments for certain fuels, and the first use of dual smog chambers to characterize the chemical evolution of smoke during simulated aging.

For tropical peat (a major global fuel type) there is very little data even after we quadrupled the number of samples burned as part of FLAME-4. Significant differences in EF between FLAME-4 Kalimantan peat and Sumatran peat from Christian et al. (2003) include ~14 times greater $NH_3$ emission from the Sumatran peat even though each study reported similar nitrogen contents (2.12% and 2.27%). Other emissions were also variable from Canadian, North Carolina, and Indonesian peat. These variable emissions could reflect differences in sampling depth; chemical, microbial, and physical weathering; drying and ignition methods, and land-use history. This highlights the need for field measurements and underscores the challenge of developing robust emissions data for this fuel type. Despite the high variability, the large increase in sampling should increase confidence in the mean emission factors for this fuel type. In addition, in all the lab peat fires studied, the emissions of HCN, $NH_3$, and $CH_4$ were elevated in comparison to the average for other types of biomass burning.

Emissions were quantified for open-cooking fires and several improved cooking stoves. We obtained good agreement for the few species that were also measured in a major cook-stove performance study indicating that our far more detailed emissions characterization in FLAME-4 can be closely linked to the performance results. This should enable a more comprehensive assessment of the economic and air quality issues associated with cooking technology options. Some of the gas-phase species (HONO, HCN, $NO_x$, glycolaldehyde, furan, and $SO_2$) are reported for “rocket” stoves (a common type of improved stove) for the first time and this emission data can be used directly without an adjustment procedure. A large set of EF for gasifier type stoves is also reported for the first time. We report the first $\Delta HCN/\Delta CO$ ER for open cooking fires, which dominate global biofuel use. The low HCN/CO

ER from cooking fires and the high HCN/CO ER from peat fires should be factored into any source apportionment based on using HCN as a tracer in regions featuring one or both types of burning.

We report the first extensive set of trace gas EF for US crop residue fires, which account for the largest burned area in the US. We report detailed EF for burning rice straw from the US and several Asian countries where this is a major pollution source. Burning food crop residues produced clearly different emissions from feed crop residues. Feed crop residues had high N-content and burning alfalfa produced the highest $NH_3$ emissions of any FLAME-4 fire. Burning sugarcane produced the highest emissions of glycolaldehyde and several other oxygenated organic compounds, possibly related to high sugar content. Increased knowledge of agricultural fire emissions should improve atmospheric modeling at local to global scales.

In general, for a wide variety of biomass fuels, the emissions of HCl are positively correlated with fuel Cl-content and MCE and larger than assumed in previous inventories. The HCl emissions are large enough that it could be the main chlorine-containing gas in very fresh smoke, but partitioning to the aerosol could be rapid. The emission factors of HCl and $SO_2$ for most crop residue and grass fires were elevated above the study average for these two gases consistent with their generally higher fuel Cl/S and tendency to burn by flaming combustion. The linkage observed between fuel chemistry or specific crops and the resulting emissions illustrates one advantage of lab-based emissions research. In contrast, our laboratory simulation of garbage burning in FLAME-4 returned an EF(HCl) (1.52 g $kg^{-1}$) near the lower end of actual landfill fire measurements (1.65 g $kg^{-1}$), possibly because a large fraction of the added polyvinyl chloride did not burn. Lower N-emissions from lab garbage burning than in Mexican landfills could be linked to missing N in our waste simulation, but we don't have nitrogen analysis of authentic waste to verify this. The average $SO_2$ EF from burning shredded tires was by far the highest for all FLAME-4 fuels at 26.2 g $kg^{-1}$. High $SO_2$ emissions together with high EF for $NO_x$ and HONO are consistent with high sulfur and nitrogen content of tires and a tendency to burn by flaming combustion. Finally, we note that this paper gives an overview of the FLAME-4 experiment and the trace gas results from OP-FTIR alone. Much more data on emissions and smoke properties will be reported separately.

**Acknowledgements**

FLAME-4, C. S. and R. Y. were supported primarily by NSF grant ATM-0936321. S. K., P. D., and FSL operational costs were supported by NASA Earth Science Division Award NNX12AH17G. A. L. R. and R. C. S. operational costs were supported by NSF grant AGS-1256042, and the DOE ASR program (ER65296). Funding for collection of Indonesian peat samples was provided by the US Department of State-US Forest Service Partnership on Indonesia's Peatlands and Climate Change in collaboration with the Kalimantan Forest and Climate Partnership. We would like to thank SANParks Scientific Services, particularly Navashni Govender, for allowing us to collect samples at the long term burn plots in KNP. We appreciate the efforts of Eric Miller, David Weise, Christine Wiedinmyer, Greg Askins, Ted Christian, Chao Wei Yu, Guenter Engling, Savitri Garivait, Christian L'Orange, Mike Hamilton, Elizabeth Stone, Emily Lincoln, Kary Peterson, Benjamin Legendre, and Brian Jenkins to harvest the fuels for this study.

858 **References**


859 Akagi, S. K., Yokelson, R. J., Wiedinmyer, C., Alvarado, M. J., Reid, J. S., Karl, T., Crounse, J. D., and Wennberg,
860 P. O.: Emission factors for open and domestic biomass burning for use in atmospheric models, Atmos. Chem. Phys.,
861 11, 4039–4072, doi:10.5194/acp-11-4039-2011, 2011.

862 Akagi, S. K., Craven, J. S., Taylor, J.W., McMeeking, G. R., Yokelson, R. J., Burling, I. R., Urbanski, S. P., Wold,
863 C. E., Seinfeld, J. H., Coe, H., Alvarado, M. J., and Weise, D. R.: Evolution of trace gases and particles emitted by a
864 chaparral fire in California, Atmos. Chem. Phys., 12, 1397–1421, doi:10.5194/acp-12-1397- 2012, 2012.

865 Akagi, S. K., Yokelson, R. J., Burling, I. R., Meinardi, S., Simpson, I., Blake, D. R., McMeeking, G. R., Sullivan,
866 A., Lee, T., Kreidenweis, S., Urbanski, S., Reardon, J., Griffith, D. W. T., Johnson, T. J., Weise, D. R.:
867 Measurements of reactive trace gases and variable $O_3$ formation rates in some South Carolina biomass burning
868 plumes, Atmos. Chem. Phys., 13, 1141-1165, doi:10.5194/acp-13-1141-2013, 2013.

869 Akagi, S. K., Burling, I. R., Mendoza, A., Johnson, T. J., Cameron, M., Griffith, D. W. T., Paton-Walsh, C., Weise,
870 D. R., Reardon, J., Yokelson, R. J.: Field measurements of trace gases emitted by prescribed fires in southeastern US
871 pine forests using an open-path FTIR system, Atmos. Chem. Phys., 14, 199-215, doi:10.5194/acp-14-199-2014,
872 2014.

873 Alvarado, M. J. and Prinn, R. G.: Formation of ozone and growth of aerosols in young smoke plumes from biomass
874 burning: 1. Lagrangian parcel studies, J. Geophys. Res., 114, D09306, doi:10.1029/2008JD011144, 2009.

875 Andreae, M. O. and Merlet, P.: Emission of trace gases and aerosols from biomass burning, Global Biogeochem.
876 Cy., 15(4), 955–966, doi:10.1029/2000GB001382, 2001.

877 Andreae, M. O. and Ramanathan, V.: Climate's dark forcings, Science, 340, 280-281, doi:10.1126/science.1235731,
878 2013.

879 Aurell, J., Gullet, B. K., and Yamamoto, D.: Emissions from open burning of simulated military waste from forward
880 operating bases, Environ. Sci. Technol., 46, 11004-11012, DOI: 10.1021/es303131k, 2012.

881 Ballhorn, U., Siegert, F., Mason, M., and Limin, S.: Derivation of burn scar depths and estimation of carbon
882 emissions with LIDAR in Indonesian peatlands, PNAS, 106(50), 21213–21218, 2009.

883 Bateman, A. P., Nizkorodov, S. A., Laskin, J., and Laskin, A.: High-resolution electrospray ionization mass
884 spectrometry analysis of water-soluble organic aerosols collected with a particle into liquid sampler, Anal. Chem.,
885 82, 8010-8016, doi:10.1021/ac1014386, 2010.

886 Becker, S., Halsall, C. J., Tych, W., Kallenborn, R., Schlabach, M., and Manø, S.: Changing sources and
887 environmental factors reduce the rates of decline of organochlorine pesticides in the Arctic atmosphere, Atmos.
888 Chem. Phys., 12, 4033-4044, doi:10.5194/acp-12-4033-2012, 2012.

Bertschi, I. T., Yokelson, R. J., Ward, D. E., Christian, T. J., and Hao, W. M.: Trace gas emissions from the production and use of domestic biofuels in Zambia measured by open-path Fourier transform infrared spectroscopy, J. Geophys. Res., 108(D13), 8469, doi:10.1029/2002JD002158 , 2003a.

Bertschi, I. T., Yokelson, R. J., Ward, D. E., Babbitt, R. E., Susott, R. A., Goode, J. G., and Hao, W. M.: Trace gas and particle emissions from fires in large diameter and belowground biomass fuels, J. Geophys. Res., 108(D13), 8472, doi:10.1029/2002JD002100, 2003b.

Biswell, H.: Prescribed Burning in California Wildlands Vegetation Management, University of California Press, Berkeley, CA, USA, 255 pp., 1999.

Bond, T. C., Streets, D. G., Yarber, K. F., Nelson, S. M., Woo, J.-H., and Klimont, Z.: A technology-based global inventory of black and organic carbon emissions from combustion, J. Geophys. Res., 109, D14203, doi:10.1029/2003JD003697, 2004.

Bond, T. C., Doherty, S. J., Fahey, D.W., Forster, P. M., Berntsen, T., DeAngelo, B. J., Flanner, M. G.,Ghan, S., Kärcher, B., Koch, D., Kinne, S., Kondo, Y., Quinn, P. K., Sarofim, M. C., Schultz, M. G., Schulz, M., Venkataraman, C., Zhang, H., Zhang, S., Bellouin, N., Guttikunda, S. K., Hopke, P. K., Jacobson, M. Z., Kaiser, J. W. , Klimont, Z., Lohmann, U., Schwarz, J. P., Shindell, D., Storelvmo, T., Warren, S. G., and Zender, C. S.: Bounding the role of black carbon in the climate system: A scientific assessment, J. Geophys. Res., 118, 5380-5552, doi:10.1002/jgrd.50171, 2013.

Bryden, M., Still, D., Scott, P., Hoffa, G., Ogle, D., Bailis, R., and Goyer, K.: Design Principles for Wood Burning Cookstoves, U.S. Environmental Protection Agency, Office of Air and Radiation, Washington DC, 2005.

Burling, I. R., Yokelson, R. J., Griffith, D. W. T., Johnson, T. J., Veres, P., Roberts, J. M., Warneke, C., Urbanski, S. P., Reardon, J., Weise, D. R., Hao, W. M., and de Gouw, J.: Laboratory measurements of trace gas emissions from biomass burning of fuel types from the southeastern and southwestern United States, Atmos. Chem. Phys., 10, 11115–11130, doi:10.5194/acp-10-11115-2010, 2010.

Burling, I. R., Yokelson, R. J., Akagi, S. K., Urbanski, S. P., Wold, C. E., Griffith, D. W. T., Johnson, T. J., Reardon, J., and Weise, D. R.: Airborne and ground-based measurements of the trace gases and particles emitted by prescribed fires in the United States, Atmos. Chem. Phys., 11, 12197–12216, doi:10.5194/acp-11-12197-2011, 2011.

Chang, D. and Song, Y.: Estimates of biomass burning emissions in tropical Asia based on satellite-derived data, Atmos. Chem. Phys., 10, 2335-2351, doi:10.5194/acp-10-2335-2010, 2010.

Christian, T., Kleiss, B., Yokelson, R. J., Holzinger, R., Crutzen, P. J., Hao, W. M., Saharjo, B. H., and Ward, D. E.: Comprehensive laboratory measurements of biomass-burning emissions: 1. Emissions from Indonesian, African, and other fuels, J. Geophys. Res., 108, 4719, doi:10.1029/2003JD003704, 2003.

Christian, T. J., Kleiss, B., Yokelson, R. J., Holzinger, R., Crutzen, P. J., Hao, W. M., Shirai, T., and Blake, D. R.: Comprehensive laboratory measurements of biomass-burning emissions: 2. First intercomparison of open path FTIR, PTR-MS, GC-MS/FID/ECD, J. Geophys. Res., 109, D02311, doi:10.1029/2003JD003874, 2004.

Christian, T. J., Yokelson, R. J., Cárdenas, B., Molina, L. T., Engling, G., and Hsu, S.-C.: Trace gas and particle emissions from domestic and industrial biofuel use and garbage burning in central Mexico, Atmos. Chem. Phys., 10, 565–584, doi:10.5194/acp-10-565-2010, 2010.

Costner, P.: Estimating Releases and Prioritizing Sources in the Context of the Stockholm Convention: Dioxin Emission Factors for Forest Fires, Grassland and Moor Fires, Open Burning of Agricultural Residues, Open Burning of Domestic Waste, Landfill and Dump Fires, The International POPs Elimination Project, Mexico, 40, 2005.

Crounse, J. D., DeCarlo, P. F., Blake, D. R., Emmons, L. K., Campos, T. L., Apel, E. C., Clarke, A. D., Weinheimer, A. J., McCabe, D. C., Yokelson, R. J., Jimenez, J. L., and Wennberg, P. O.: Biomass burning and urban air pollution over the Central Mexican Plateau, Atmos. Chem. Phys., 9, 4929–4944, doi:10.5194/acp-9-4929-2009, 2009.

Crutzen, P. J. and Andreae, M. O.: Biomass burning in the tropics: Impact on atmospheric chemistry and biogeochemical cycles, Science, 250, 1669–1678, doi:10.1126/science.250.4988.1669, 1990.

Eckhardt, S., Breivik, K., Manø, S., Stohl, A.: Record high peaks in PCB concentrations in the Arctic atmosphere due to long-range transport of biomass burning emissions, Atmos. Chem. Phys., 7, 4527-4536, doi:10.5194/acp-7-4527-2007, 2007.

Ferek, R. J., Reid, J. S., Hobbs, P. V., Blake, D. R., and Liousse, C.: Emission factors of hydrocarbons, halocarbons, trace gases, and particles from biomass burning in Brazil, J. Geophys. Res., 103(D24), 32107–32118, doi:10.1029/98JD00692, 1998.

Forster, P., Ramaswamy, V., Artaxo, P., Berntsen, T., Betts, R., Fahey, D. W., Haywood, J., Lean, J., Lowe, D. C., Myhre, G., Nganga, J., Prinn, R., Raga, G., Schulz, M., and Van Dorland, R.: Radiative Forcing of Climate Change, in Climate Change 2007: The Physical Science Basis. Contribution of Working Group I to the Fourth Assessment Report of the Intergovernmental Panel on Climate Change, edited by S. Solomon, D. Qin, M. Manning, Z. Chen, M. Marquis, K. B. Averyt, M. Tignor, and H. L. Miller, pp. 129–234, Cambridge Univ. Press, Cambridge, United Kingdom and New York, NY, USA, 2007.

Goode, J. G., Yokelson, R. J., Susott, R. A., and Ward, D. E.: Trace gas emissions from laboratory biomass fires measured by Fourier transform infrared spectroscopy: Fires in grass and surface fuels, J. Geophys. Res., 104, 21237 – 21 245, doi:10.1029/1999JD900360, 1999.

Govender, N., Trollope, W. S. W, and van Wilgen, B. W.: The effect of fire season, fire frequency, rainfall and management on fire intensities in savanna vegetation in South Africa, J. Appl. Ecol., 43, 748–758, doi: 10.1111/j.1365-2664.2006.01184.x, 2006.

Gras, J. L., Jensen, J. B., Okada, K., Ikegami, M., Zaizen, Y., and Makino, Y.: Some optical properties of smoke aerosol in Indonesia and tropical Australia, Geophys. Res. Lettr. 26, 1393-1396, doi: 10.1029/1999GL900275, 1999.

Grieshop, A. P., Logue, J. M., Donahue, N. M., and Robinson, A. L.: Laboratory investigation of photochemical oxidation of organic aerosol from wood fires 1: measurement and simulation of organic aerosol evolution, Atmos. Chem. Phys., 9, 1263–1277, doi:10.5194/acp-9-1263-2009, 2009.

Griffith, D. W. T., Mankin, W. G., Coffey, M. T., Ward, D. E., and Riebau, A.: FTIR remote sensing of biomass burning emissions of $CO_2$, CO, $CH_4$, $CH_2O$, NO, $NO_2$, $NH_3$, and $N_2O$, in: Global Biomass Burning: Atmospheric, Climatic, and Biospheric Implications, edited by: Levine, J. S., MIT Press, Cambridge, 230–239, 1991.

Griffith, D. W. T.: Synthetic calibration and quantitative analysis of gas phase infrared spectra, Appl. Spectrosc., 50, 59–70, 1996.

Hardy, C. C., Conard, S. G., Regelbrugge, J. C., and Teesdale, D. R.: Smoke emissions from prescribed burning of southern California chaparral, Res. Pap. PNW-RP-486, US Department of Agriculture, Forest Service, Pacific Northwest Research Station, Portland, OR, 1996.

Hatch, L. E., Luo, W., Pankow, J. F., Yokelson, R. J., Stockwell, C. E., and Barsanti, K. C.: Identification and quantification of gaseous organic compounds emitted from biomass burning using two-dimensional gas chromatography/time-of-flight mass spectrometry, in prep., 2014.Hennigan, C. J., Miracolo, M. A., Engelhart, G. J., May, A. A., Presto, A. A., Lee, T., Sullivan, A. P., McMeeking, G. R., Coe, H., Wold, C.E., Hao, W. M., Gilman, J. B., Kuster, W. C., de Gouw, J., Schichtel, B. A., Collett Jr., J. L., Kreidenweis, S. M., and Robinson, A. L.: Chemical and physical transformations of organic aerosol from the photo-oxidation of open biomass burning emissions in an environmental chamber, Atmos. Chem. Phys., 11, 7669-7686, doi:10.5194/acp-11-7669-201, 2011.

IPCC, 2006: 2006 IPCC Guidelines for National Greenhouse Gas Inventories, prepared by the National Greenhouse Gas Inventories Programme, edited by: Eggleston, H. S., Buendia, L.,Miwa, K., Ngara, T., and Tanabe, K., Institute for Global Environmental Strategies (IGES), Hayama, Japan, 2006.

Jetter, J., Zhao, Y., Smith, K. R., Khan, B., Yelverton, T., DeCarlo, P., and Hays, M. D.: Pollutant emissions and energy efficiency under controlled conditions for household biomass cookstoves and implications for metrics useful in setting international test standards, Environ. Sci. Technol., 46, 10827-10834, doi:10.1021/es301693f , 2012.

Johnson, T. J., Disselkamp, R. S., Su, Y.-F., Fellows, R. J., Alexander, M. L., and Driver, C. J.: Gas-Phase Hydrolysis of SOCl2 at 297 and 309 K: Implications for Its Atmospheric Fate, J. Phys. Chem. A, 107, 6183–6190, doi:10.1021/jp022090v, 2003.

Johnson, T. J., Masiello, T., and Sharpe, S. W.: The quantitative infrared and NIR spectrum of CH2I2 vapor: vibrational assignments and potential for atmospheric monitoring, Atmos. Chem. Phys., 6, 2581–2591, doi:10.5194/acp-6-2581-2006, 2006.

Johnson, M., Edwards, R., Frenk, C. A., and Masera, O.: Infield greenhouse gas emissions from cookstoves in rural Mexican households, Atmos. Environ. 42, 1206–1222, 2008.

Johnson, T. J., Profeta, L. T. M., Sams, R. L., Griffith, D.W. T., and Yokelson, R. L.: An infrared spectral database for detection of gases emitted by biomass burning, Vib. Spectrosc., 53, 97–102, doi:10.1016/j.vibspec.2010.02.010, 2010.

Johnson, T. J., Sams, R. L., Profeta, L. T. M., Akagi, S. K., Burling, I. R., Williams, S. D., and Yokelson, R. J.: Quantitative IR spectrum and vibrational assignments for glycolaldehyde: Application to measurements in biomass burning plumes, J. Phys. Chem. A, 117, 4096-4107, doi:10.1021/jp311945p, 2013.

Keene, W. C., M. A. K. Khalil, D. J. Erickson III, A. McCulloch, T. E. Graedel, J. M. Lobert, M. L. Aucott, S. L. Gong, D. B. Harper, G. Kleiman, P. Midgley, R. M. Moore, C. Seuzaret, W. T. Sturges, C. M. Benkovitz, V. Koropalov, L. A. Barrie, and Y. F. Li, Composite global emissions of reactive chlorine from anthropogenic and natural sources: Reactive Chlorine Emissions Inventory, J. Geophys. Res., 104, 8429 – 8440, 1999.

Keene, W. C., Lobert, J. M., Crutzen, P. J., Maben, J. R., Scharffe, D. H., and Landmann, T.: Emissions of major gaseous and particulate species during experimental burns of southern African biomass, J. Geophys. Res., 111, D04301, doi:10.1029/2005JD006319, 2006.

Kirchstetter, T. W., Novakov, T., and Hobbs, P. V.: Evidence that the spectral dependence of light absorption by aerosols is affected by organic carbon, J. Geophys. Res., 109, D21208, doi:10.1029/2004JD004999, 2004.

Knapp, E. E., Estes, B. L., and Skinner, C.N.: Ecological effects of prescribe fire season: a literature review and synthesis for managers, Gen. Tech. Rep., PSW-GTR-224, Department of Agriculture, Forest service, Alabany, CA, 2009.

Komazaki, Y., Hashimoto, S., Inoue, T., and Tanaka, S.: Direct collection of $HNO_3$ and HCl by a diffusion scrubber without inlet tubes, Atmos. Environ., 36, 1241–1246, doi:10.1016/S1352-2310(01)00571-4, 2002.

1007 Lara, L. L., Artaxo, P., Martinelli, L. A., Camargo, P. B., Victoria, R. L., and Ferraz, E. S. B.: Properties of aerosols
1008 from sugarcane burning emissions in Southeastern Brazil, Atmos. Environ., 39, 4627–4637,
1009 doi:10.1016/j.atmosenv.2005.04.026, 2005.

1010 Lehmann, C. M. B. and Gay, D. A.: Monitoring long-term trends of acidic wet deposition in US precipitation:
1011 Results from the National Atmospheric Deposition Program, Power Plant Chem., 13, 386–393, 2011.

1012 Lei, W., Li, G., and Molina, L. T.: Modeling the impacts of biomass burning on air quality in and around Mexico
1013 City, Atmos. Chem. Phys., 13, 2299-2319, doi:10.5194/acp-13-2299-2013, 2013.

1014 Lemieux, P. M.: Evaluation of Emissions from the Open Burning of Household Waste in Barrels, EPA/600/SR-
1015 97/134, United States Environmental Protection Agency, Office of Research and Development, Washington DC,
1016 1998.

1017 Lemieux, P.M., Lutes, C.C., Abbott, J.A., and Aldous, K.M.: Emissions of Polychlorinated Dibenzo-p-dioxins and
1018 Polychlorinated Dibenzofurans from the Open Burning of Household Waste in Barrels, Environ.Sci. Technol., 34
1019 (3), 377-384, doi:10.1021/es990465t, 2000.

1020 Lemieux, P. M., Gullett, B.K., Lutes, C.C., Winterrowd, C. K., Winters, D. L.: Variables affecting emissions of
1021 PCDD/Fs from uncontrolled combustion of household waste in barrels, J. Air Waste Manage. Assoc., 53, 523-531,
1022 doi: 10.1080/10473289.2003.10466192, 2003.

1023 Levin, E. J. T., McMeeking, G. R., Carrico, C. M., Mack, L. E., Kreidenweis, S. M., Wold, C. E., Moosmüller, H.,
1024 Arnott, W. P., Hao, W. M., Collett Jr., J. L., and Malm, W. C.: Biomass burning smoke aerosol properties measured
1025 during Fire Laboratory at Missoula Experiments (FLAME), J. Geophys. Res., 115, D18210,
1026 doi:10.1029/2009JD013601, 2010.

1027 Levin, E. J. T., McMeeking, G. R., DeMott, P. J., McCluskey, C. S., Stockwell, C. E., Yokelson, R. J., and
1028 Kreidenweis, S. M.: A new method to determine the number concentrations of refractory black carbon ice nucleating
1029 particles, Aerosol Sci. Technol., submitted, 2014.

1030 Li, G., Lei, W., Bei, N., and Molina, L. T.: Contribution of garbage burning to chloride and $PM_{2.5}$ in Mexico City,
1031 Atmos. Chem. Phys., 12, 8751-8761, doi :10.5194/acp-12-8751-2012, 2012.

1032 Li, Q., Jacob, D. J., Bey, I., Yantosca, R. M., Zhao, Y., Kondo, Y., and Notholt, J.: Atmospheric hydrogen cyanide
1033 (HCN): biomass burning source, ocean sink?, Geophys. Res. Lett., 27(3), 357–360, 2000.

1034 Li, J., Posfai, M., Hobbs, P. V and Buseck, P. R.: Individual aerosol particles from biomass burning in southern
1035 Africa: 2. Compositions and aging of inorganic particles, J. Geophys. Res., 108, 8484, doi:10.1029/2002JD002310,
1036 2003.

1037 Lin, P., Engling, G., and Yu, J. Z.: Humic-like substances in fresh emissions of rice straw burning and in ambient
1038 aerosols in the Pearl River Delta Region, China, Atmos. Chem. Phys., 10, 6487-6500, doi:10.5194/acp-10-6487-
1039 2010, 2010.

1040 Liu, S., Aiken, A. C., Arata, C., Manvendra, K. D., Stockwell, C. E., Yokelson, R. J., Stone, E. A., Jayarathne, T.,
1041 Robinson, A. L., DeMott, P. J., and Kreidenweis, S. M.: Aerosol single scattering albedo dependence on biomass
1042 combustion efficiency: Laboratory and field studies, Geophys. Res. Lett., 41, 742-748, doi:10.1002/2013GL058392,
1043 2014.

1044 Lobert, J. M., Scharffe, D. H., Hao, W. M., Kuhlbusch, T. A., Seuwen, R., Warneck, P., and Crutzen, P. J.:
1045 Experimental evaluation of biomass burning emissions: Nitrogen and carbon containing compounds, in: Global
1046 Biomass Burning: Atmospheric, Climatic, and Biospheric Implications, Levine, J. S., MIT Press, Cambridge, 289–
1047 304, 1991.

1048 Lobert, J. M., Keene, W. C., Logan, J. A., and Yevich, R.: Global chlorine emissions from biomass burning:
1049 Reactive Chlorine Emissions Inventory, J. Geophys. Res., 104, 8373–8389, doi:10.1029/1998jd100077, 1999.

1050 L'Orange, C., Volckens, J., and DeFoort, M.: Influences of stove type and cooking pot temperature on particulate
1051 matter emissions from biomass cook stoves, Energy Sustainable Dev., 16, 448-455, doi: 10.1016/j.esd.2012.08.008,
1052 2012a.

1053 L'Orange, C., DeFoort, M., and Willson, B.: Influence of testing parameters on biomass stove performance and
1054 development of an improved testing protocol, Energy Sustainable Dev., 16, 3-12, doi:10.1016/j.esd.2011.10.008,
1055 2012b.

1056 MacCarty, N., Ogle, D., Still, D., Bond, T., and Roden, C.: A laboratory comparison of the global warming impact
1057 of five major types of biomass cooking stoves, Energy Sustainable Dev., 12, 5−14, 2008.

1058 Marlier, M. E., DeFries, R. S., Voulgarakis, A., Kinney, P. L., Randerson, J. T., Shindell, D. T., Chen, Y., and
1059 Faluvegi, G.: El Niño and health risks from landscape fire emissions in southeast Asia, Nature Climate Change, 3,
1060 131-136, doi:10.1038/nclimate1658, 2013.

1061 Martínez, J. D., Puy, N., Murillo, R., Garciá, T., Navarro, M. V., and Mastral, A. M.: Waste tyre pyrolysis- A
1062 review, Renewable Sustainable Energy Rev., 23, 179-213, doi:10.1016/j.rser.2013.02.038, 2013.

Mastral, A. M., Murillo, R., Callen, M. S., Garcia, T., and Snape, C. E.: Influence of process variables on oils from tire pyrolysis and hydropyrolysis in a swept fixed bed reactor, Energy & Fuels, 14(4), 739-744, doi:10.1021/ef990183e, 2000.

McCarty,J. L., Justice, C. O., and Korontzi, S.: Agricultural burning in Southeastern United States detected by MODIS, Remote Sen. Environ., 108, 151-162, doi:10.1016/j.rse.2006.03.020, 2007.

McCarty, J. L., Korontzi, S., Justice, C. O., and Loboda, T.: The spatial and temporal distribution of crop residue burning in the contiguous United States, Sci. Total Environ., 407, 5701-5712, doi: 10.1016/j.scitotenv.2009.07.009, 2009.

McCulloch, A., Aucott, M. L., Benkovitz, C. M., Graede, T. E., Kleiman, G., Midgley, P. M., and Li, Y. F.: Global emissions of hydrogen chloride and chloromethane from coal combustion, incineration and industrial activities: Reactive Chlorine Emissions Inventory, J. Geophys. Res., 104(D7), 8391–8403, 1999.

McKenzie, L.M., Ward, D. E., Hao, W. M.: Chlorine and bromine in the biomass of tropical and temperate ecosystems, Biomass Burning and Global Change, vol. 1, Remote Sensing, Modeling and Inventory Development, and Biomass Burning in Africa., J. S. Levine, 241-248, MIT Press, Cambridge, Massachusetts, 241-248, 1996.

McMeeking, G. R., Kreidenweis, S. M., Baker, S., Carrico, C. M., Chow, J. C., Collet Jr., J. L., Hao, W. M., Holden, A. S., Kirchstetter, T. W., Malm, W. C., Moosmüller, H., Sullivan, A. P., and Wold, C. E.: Emissions of trace gases and aerosols during the open combustion of biomass in the laboratory, J. Geophys. Res., 114, D19210, doi:10.1029/2009JD011836, 2009.

Melvin, M. A.: 2012 national prescribed fire use survey report, Technical Report 01-12, Coalition of Prescribed Fire Councils, Inc., 1–19, 2012.

Nyman, J. A. and Chabreck, R. H.: Fire in coastal marshes: history and recent concerns, Fire in the wetlands: a management perspective, in: Tall Timbers Fire Ecology Conference 19th Proceedings, Tallahassee, FL, 134–141, 1995

Oanh, N. T. K., Bich, T. L., Tipayarom, D., Manadhar, B. R., Prapat, P., Simpson, C. D., and Liu, L.-J. S.: Characterization of particulate matter emission from open burning of rice straw, Atmos. Environ., 45, 493–502, 2011.

OCIA: Organisation Internationale des Constructeurs d'Automobiles http://www.oica.net/category/production-statistics/, last access: 31 October 2013, 2013.

1091 Ortiz-Montalvo, D. L., Lim, Y. B., Perri, M .J., Seitzinger, S. P., Turpin, B. J.: Volatility and Yield of
1092 Glycolaldehyde SOA formed through Aqueous Photochemistry and Droplet Evaporation, Aerosol Sci. Technol., 46,
1093 1002−1014, doi:10.1080/02786826.2012.686676, 2012.

1094 Page, S. E., Siegert, F., Rieley, J. O., Boehm, H. D. V., Jaya, A., and Limin, S.: The amount of carbon released from
1095 peat and forest fires in Indonesia during 1997, Nature, 420, 61–65, doi:10.1038/nature01131, 2002.

1096 Park, R. J., Jacob, D. J., and Logan, J. A.: Fire and biofuel contributions to annual mean aerosol concentrations in
1097 the United States, Atmos. Environ., 41, 7389–7400, 2007.

1098 Parker, L. and Blodgett, J.: Greenhouse Gas Emissions: Perspectives on the Top 20 Emitters and Developed versus
1099 Developing Nations, Congressional Research Service (CRS) Report for Congress, RL32721, Washington DC, 2008.

1100 Pehlken, A. and Essadiqi, E.: Scrap tire recycling in Canada CANMET-MCL, Report for Natural Resources Canada,
1101 Ottawa, Canada, MTL 2005-08(CF), 2005.

1102 Petters, M. D., M. T. Parsons, A. J. Prenni, P. J. DeMott, S. M. Kreidenweis, C. M. Carrico, A. P. Sullivan, G. R.
1103 McMeeking, E. Levin, C. E. Wold, J. L. Collett, Jr., and H. Moosmüller: Ice nuclei emissions from biomass burning,
1104 J. Geophys. Res., 114, D07209, doi: 10.1029/2008JD011532, 2009.

1105 Radke, L. F., Hegg, D. A., Hobbs, P. V., Nance, J. D., Lyons, J. H., Laursen, K. K., Weiss, R. E., Riggan, P. J. and
1106 Ward, D. E.: Particulate and trace gas emissions from large biomass fires in North America, in Global Biomass
1107 Burning: Atmospheric, Climatic, and Biospheric Implications, Levine, J. S., MIT Press, Cambridge, MA, USA,
1108 209–224, 1991.

1109 Pratt, K. A., Murphy, S. M., Subramanian, R., DeMott, P. J., Kok, G. L., Campos, T., Rogers, D. C., Prenni, A. J.,
1110 Heymsfield, A. J., Seinfeld, J. H. and Prather, K. A.: Flight-based chemical characterization of biomass burning
1111 aerosols within two prescribed burn smoke plumes, Atmos. Chem. Phys., 11(24), 12549–12565, doi:10.5194/acp-
1112 11-12549-2011, 2011.

1113 Ramanathan, V. and Carmichael, G.: Global and regional climate changes due to black carbon, Nature Geoscience,
1114 1, 221-227, doi:10.1038/ngeo156, 2008.

1115 Randerson, J. T., van der Werf, G. R., Collatz, G. J., Giglio, L., Still, C. J., Kasibhatla, P., Miller, J. B., White, J. W.
1116 C., De-Fries, R. S., and Kasischke, E. S.: Fire emissions from C3 and C4 vegetation and their influence on
1117 interannual variability of atmospheric CO2 and d13CO2, Global Biogeochem. Cy., 19, GB2019,
1118 doi:10.1029/2004GB002366, 2005.

Randerson, J. T., Chen, Y., van der Werf, G. R., Rogers, B. M., and Morton, D. C.: Global burned area and biomass burning emissions from small fires, J. Geophys. Res., 117, G04012, doi:10.1029/2012JG002128, 2012.

Rappold, A. G., Stone, S. L., Cascio, W. E., Neas, L. M., Kilaru, V. J., Carraway, M. S., Szykman, J. J., Ising, A., Cleve, W. E., Meredith, J. T., Vaughan-Batten, H., Deyneka, L., and Devlin. R. B.: Peat bog wildfire smoke exposure in rural North Carolina is associated with cardiopulmonary emergency department visits assessed through syndromic surveillance, Environ. Health Perspect., 119, 1415–1420, 2011.

Reid, J. S., Hobbs, P. V., Ferek, R. J., Martins, J. V., Blake, D. R., Dunlap, M. R., and Liousse, C.: Physical, chemical, and radiative characteristics of the smoke dominated regional hazes over Brazil, J. Geophys. Res., 103, 32059–32080, doi:10.1029/98JD00458, 1998.

Reid, J. S., Hyer, E. J., Johnson, R., Holben, B. N., Yokelson, R. J., Zhang, J., Campbell, J. R., Christopher, S. A., Di Girolamo , L., Giglio, L., Holz, R. E., Kearney, C., Miettinen, J., Reid, E. A., Turk, F. J., Wang, J., Xian, P., Zhao, G., Balasubramanian, R., Chew, B. N., Janai, S., Lagrosas, N., Lestari, P., Lin, N.-H., Mahmud, M.. Nguyen, A. X., Norris, B., Oahn, N. T.K., Oo, M., Salinas, S. V., Welton, E. J., Liew, S. C.: Observing and understanding the Southeast Asian aerosol system by remote sensing: An initial review and analysis for the Seven Southeast Asian Studies (7SEAS) program, Atmos. Res., 122, 403-468, doi:10.1016/j.atmosres.2012.06.005, 2013.

RMA: U.S. Scrap tire management summary, Rubber Manufacturers Association, Washington DC, available at: http://www.rma.org/download/scrap-tires/market-reports/US_STMarkets2009.pdf (last access: April 9, 2014), 2011.

Roden, C. A., Bond, T. C., Conway, S., Pinel, A. B. O., MacCarty, N., and Still, D. Laboratory and field investigations of particulate and carbon monoxide emissions from traditional and improved cookstoves, Atmos. Environ., 43, 1170−1181, doi:10.1016/j.atmosenv.2008.05.041, 2008.

Rohr, A. C., and Wyzga, R. E.: Attributing health effects to individual particulate matter constituents, Atmos. Environ., 62, 130-152, 2012.

Roth, C.: Micro-Gasification: Cooking with Gas from Biomass, Deutsche Gesellschaft fur Internationalle Zusammenarbeit (GIZ) GmbH, Eschborn, Germany, 2011.

Rothman, L. S., Gordon, I. E., Barbe, A., Benner, D. C., Bernath, P. F., Birk, M., Boudon, V., Brown, L. R., Campargue, A., Champion, J. P., Chance, K., Coudert, L. H., Dana, V., Devi, V. M., Fally, S., Flaud, J. M., Gamache, R. R., Goldman, A., Jacquemart, D., Kleiner, I., Lacome, N., Lafferty, W. J., Mandin, J. Y., Massie, S. T., Mikhailenko, S. N., Miller, C. E., Moazzen-Ahmadi, N., Naumenko, O. V., Nikitin, A. V., Orphal, J., Perevalov, V. I., Perrin, A., Predoi-Cross, A., Rinsland, C. P., Rotger, M., Simeckov´a, M., Smith, M. A. H., Sung, K., Tashkun, S. A., Tennyson, J., Toth, R. A., Vandaele, A. C., and Vander Auwera, J.: The HITRAN 2008 molecular spectroscopic database, J. Quant. Spectrosc. Ra., 110, 533–572, doi:10.1016/j.jqsrt.2009.02.013, 2009.

Saleh, R., Robinson, E. S., Tkacik, D., Ahern, A., Liu, S., Aiken, A., Sullivan, R., Presto, A. A., Dubey, M. K., Yokelson, R. J., Donahue, N. M., and Robinson, A. L.: Light absorption by biomass-burning aerosols: Brownness of organics scales with black carbon content, accepted, Nat. Geosci., 2014.

Schiller, C.L., Locquiao, S., Johnson, T.J., Harris, G.W.: Atmospheric measurements of HONO by tunable diode laser absorption spectroscopy, Journal of Atmospheric Chemistry, 40, 275–293, 2001.

Schimel, D., Alves, D., Enting, I., Heimann, M., Joos, F., Raynaud, D., Wigley, T., Prather, M., Derwent, R., Ehhalt, D., Fraser, P., Sanhueza, E., Zhou, X., Jonas, P., Charlson, R., Rodhe, H., Sadasivan, S., Shine, K. P., Fouquart, Y., Ramaswamy, V., Solomon, S., Srinivasan, J., Albritton, D., Isaksen, I., Lal, M., Wuebbles, D.: Radiative forcing of climate change: Climate Change 1995: The Science of Climate Change, Houghton J. T., Meira Filho L. G., Callander B. A., Harris N., Kattenberg, A., Maskell, K.**,** Cambridge Univ. Press, Cambridge, 1996.

Sharpe, S. W., Johnson, T. J., Sams, R. L., Chu, P. M., Rhoderick, G. C., and Johnson, P. A.: Gas-phase databases for quantitative infrared spectroscopy, Appl. Spectrosc., 58, 1452–1461, 2004.

Shea, R. W., Shea, B. W., Kauffman, J. B, Ward, D. E., Haskins, C. I., and Scholes M. C.: Fuel biomass and combustion factors associated with fires in savanna ecosystems of South Africa and Zambia, J. Geophys. Res., 101, 23,551–23,568, doi:10.1029/95JD02047, 1996.

Simoneit, B. R. T., Kobayashi, M., Mochida, M., Kawamura, K., and Huebert, B. J.: Aerosol particles collected on aircraft flights over the northwestern Pacific region during the ACE-Asia campaign: Composition and major sources of the organic compounds, J. Geophys. Res., 109, D19S09, doi:10.1029/2004JD004565, 2004a.

Simoneit, B. R. T., Kobayashi, M., Mochida, M., Kawamura, K., Lee, M., Lim, H.-J., Turpin, B. J., and Komazaki, Y.: Composition and major sources of organic compounds of aerosol particulate matter sampled during the ACE-Asia campaign, J. Geophys. Res., 109, D19S10, doi:10.1029/2004JD004598, 2004b.

Simpson, I. J., Rowland, F. S., Meinardi, S., and Blake, D. R.: Influence of biomass burning during recent fluctuations in the slow growth of global tropospheric methane, Geophys. Res. Lett., 33, L22808, doi:10.1029/2006GL027330, 2006.

Sinha, P., Hobbs, P. V., Yokelson, R. J., Bertschi, I. T., Blake, D. R., Simpson, I. J., Gao, S., Kirchstetter, T. W., and Novakov, T.: Emissions of trace gases and particles from savanna fires in southern Africa, J. Geophys. Res., 108, 8487, doi:10.1029/2002JD002325, 2003.

Sinha, V., Kumar, V., and Sarkar, C.: Chemical composition of pre-monsoon air in the Indo-Gangetic Plain measured using a new air quality facility and PTR-MS: high surface ozone and strong influence of biomass burning, Atmos. Chem. Phys., 14, 5921-5941, doi:10.5194/acp-14-5921-2014, 2014.

Smith, K. R., Frumkin, H., Balakrishnan, K., Butler, C. D., Chafe, Z. A., Fairlie, I., Kinney, P., Kjellstrom, T., Mauzerall, D. L., McKone, T. E., McMichael, A. J., and Schneider, M.: Energy and human health, Annu. Rev. Public Health, 34, 1–25, 2013.

Smith, S.J., Pitcher, H., and Wigley, T. M. L.: Global and regional anthropogenic sulfur dioxide emissions, Global and Planetary Change, 29, 99-119, 2001.

Smith, S.J., van Aardenne, J., Klimont, Z., Andres, R. J., Volke, A., and Delgado Arias, S.: Anthropogenic sulfur dioxide emissions: 1850-2005, Atmos. Chem. Phys., 11, 1101-1116, doi:10.5194/acp-11-1101-2011, 2011.

Streets, D. G., Yarber, K. F., Woo, J. H., and Carmichael, G. R.: Biomass burning in Asia: annual and seasonal estimates and atmospheric emissions, Global Biogeochem. Cy., 17(4), 1099, doi:10.1029/2003GB002040, 2003.

Stockwell, C. E., Veres, P. R., Williams, J., and Yokelson, R. J.: Characterization of biomass burning smoke from cooking fires, peat, crop residue and other fuels with high resolution proton-transfer-reaction time-of-flight mass spectrometry, Atmos. Chem. Phys., in preparation, 2014.

Tkacik, D., et al: A dual chamber enhancement method to quantify aerosol formation: Biomass burning secondary organic aerosol, in preparation, 2014.

Thompson, A. M.: The oxidizing capacity of the Earth's atmosphere: Probable past and future changes, Science, 256(5060), 1157-1165, doi: 10.1126/science.256.5060.1157, 1992.

Trentmann, J., Yokelson, R. J., Hobbs, P. V., Winterrath, T., Christian, T. J., Andreae, M. O., and Mason, S. A.: An analysis of the chemical processes in the smoke plume from a savanna fire, J. Geophys. Res., 110, D12301, doi:10.1029/2004JD005628, 2005.

Turetsky, M. R., Kane, E. S., Harden, J. W., Ottmar, R. D., Manies, K. L., Hoy E., and Kasischke, E. S.: Recent acceleration of biomass burning and carbon losses in Alaskan forests and peatlands, Nature Geoscience, 4, 27–31, doi:10.1038/ngeo1027, 2011.

UNFPA: State of the world population 2012, E.12.III.H., Information and External Relations Division of UNFPA, United Nations Population Fund, New York, 2012.

USEPA: Air Emissions from Scrap Tire Combustion, EPA-600/R-97-115, Office of Research and Development, Washington DC, 1997.

USEPA: An inventory of sources and environmental releases of dioxin-like compounds in the United States for the years 1987, 1995, and 2000, EPA/600/P-03/002F, National Center for Environmental Assessment, Office of Research and Development, Washington, DC, 677 pp., 2006.

USEPA: Inventory of U.S. Greenhouse Gas Emissions and Sinks: 1990-2011, EPA 430-R-13-001, Office of Atmospheric Programs, Washington DC, 2013.

USEPA: Plastics, available at:http://www.epa.gov/climatechange/wycd/waste/downloads/plastics-chapter10-28-10.pdf, United States Environmental Protection Agency, (last access: 9 April 2014), 2010.

van der A, R. J., Eskes, H. J., Boersma, K. F., van Noije, T. P. C., Van Roozendael, M., De Smedt, I., Peters, D. H. M. U., and Meijer, E.W.: Trends, seasonal variability and dominant $NO_x$ source derived from a ten year record of $NO_2$ measured from space, J. Geophys. Res., 113, D04302, doi:10.1029/2007JD009021, 2008.

van der Werf, G. R., Randerson, J. T., Giglio, L., Collatz, G. J., Mu, M., Kasibhatla, P. S., Morton, D. C., DeFries, R. S., Jin, Y., and van Leeuwen, T. T.: Global fire emissions and the contribution of deforestation, savanna, forest, agricultural, and peat fires (19972009), Atmos. Chem. Phys., 10, 11707–11735, doi:10.5194/acp-10-11707-2010, 2010.

Veres, P., Roberts, J. M., Burling, I. R., Warneke, C., de Gouw, J., and Yokelson, R. J.: Measurements of gas-phase inorganic and organic acids from biomass fires by negative-ion proton-transfer chemical-ionization mass spectrometry, J. Geophys. Res., 115, D23302, doi:10.1029/2010JD014033, 2010.

Wade, D. D. and Lunsford, J. D.: A guide for prescribed fire in southern forests, USDA Forest Service Southern Region, Atlanta, GA, USA, 56 pp., 1989.

Ward, D. E. and Radke, L. F.: Emissions measurements from vegetation fires: A Comparative evaluation of methods and results, in: Fire in the Environment: The Ecological, Atmospheric and Climatic Importance of Vegetation Fires, edited by: Crutzen, P. J. and Goldammer, J. G., John Wiley, New York, 53–76, 1993.

Warneke, C., Roberts, J. M., Veres, P., Gilman, J., Kuster, W. C., Burling, I., Yokelson, R. J., de Gouw, J. A.: VOC identification and inter-comparison from laboratory biomass burning using PTR-MS and PIT-MS, Int. J. Mass Spectrom. Ion Proc., 303, 6-14, doi: 10.1016/j.ijms.2010.12.002, 2011.

Washenfelder, R. A., Flores, J. M., Brock, C. A., Brown, S. S., and Rudich, Y.: Broadband measurements of aerosol extinction in the ultraviolet spectral region, Atmos. Meas. Tech., 6, 861-877, doi:10.5194/amt-6-861-2013, 2013.

Webster, C. R., May, R. D., Trimble, C. A., Chave, R. G., and Kendall, J.: Aircraft (ER-2) laser infrared absorption spectrometer (ALIAS) for in-situ stratospheric measurements of HCI, N2O, CH4, NO2, and HNO3, Appl. Opt., 33, 454–472, doi:10.1364/AO.33.000454, 1994.

WHO: Global Health Risks: Mortality and Burden of Disease Attributable to Selected Major Risks, Department of Health Statistics and Informatics in the Information, Evidence and Research Cluster of the World Health Organization, Geneva, Switzerland, 2009.

Wiedinmyer, C., Akagi, S. K., Yokelson, R. J., Emmons, L. K., Al-Saadi, J.A., Orlando, J. J., and Soja, A.J.: The Fire INventory from NCAR (FINN): a high resolution global model to estimate the emissions from open burning, Geosci. Model Dev., 4, 625-641, doi:10.5194/gmd-4-625-2011, 2011.

Woodall, B. D., Yamamoto, D. P., Gullett, B. K., and Touati, A.: Emissions from small-scale burns of simulated deployed U.S. military waste, Environ. Sci. Technol., 46, 10997-11003, doi: 10.1021/es3021556, 2012.

Wooster, M. J., Freeborn, P. H., Archibald, S., Oppenheimer, C., Roberts, G. J., Smith, T. E. L., Govender, N., Burton, M., and Palumbo, I.: Field determination of biomass burning emission ratios and factors via open-path FTIR spectroscopy and fire radiative power assessment: headfire, backfire and residual smouldering combustion in African savannahs. Atmos. Chem. Phys., 11, 11591–11615, doi:10.5194/acp-11-11591-2011, 2011.

Worden, J., Wecht, K., Frankenberg, C., Alvarado, M., Bowman, K., Kort, E., Kulawik, S., Lee, M., Payne, V., and Worden, H.: $CH_4$ and CO distributions over tropical fires during October 2006 as observed by the Aura TES satellite instrument and modeled by GEOS-Chem, Atmos. Chem. Phys., 13(7), 3679–3692, doi:10.5194/acp-13-3679-2013, 2013.

Yevich, R. and Logan, J. A.: An assessment of biofuel use and burning of agricultural waste in the developing world, Global Biogeochem. Cy., 17(4), 1095, doi:10.1029/2002GB001952, 2003.

Yokelson, R. J., Griffith, D. W. T., and Ward, D. E.: Open path Fourier transform infrared studies of large-scale laboratory biomass fires, J. Geophys. Res., 101, 21067–21080, doi:10.1029/96JD01800, 1996.

Yokelson, R. J.,Ward, D. E., Susott, R. A., Reardon, J., and Griffith, D. W. T.: Emissions from smoldering combustion of biomass measured by open-path Fourier transform infrared spectroscopy, J. Geophys. Res., 102(D15), 18865–18877, 1997.

Yokelson, R. J., Goode, J. G., Ward, D. E., Susott, R. A., Babbitt, R. E., Wade, D. D., Bertschi, I., Griffith, D. W. T., and Hao, W. M.: Emissions of formaldehyde, acetic acid, methanol, and other trace gases from biomass fires in North Carolina measured by airborne Fourier transform infrared spectroscopy, J. Geophys. Res., 104, 30109–30125, doi:10.1029/1999jd900817, 1999.

1263 Yokelson, R. J., Bertschi, I. T., Christian, T. J., Hobbs, P. V., Ward, D. E., and Hao,W. M.: Trace gas measurements
1264 in nascent, aged, and cloud-processed smoke from African savanna fires by airborne Fourier transform infrared
1265 spectroscopy, AFTIR, with coincident measurements of aerosol optical depth, J. Geophys. Res., 108, 8478,
1266 doi:10.1029/2002JD002322, 2003a.

1267 Yokelson, R. J., Christian, T. J., Bertschi, I. T., and Hao, W. M.: Evaluation of adsorption effects on measurements
1268 of ammonia, acetic acid, and methanol, J. Geophys. Res., 108, 4649, doi:10.1029/2003JD003549, 2003b.

1269 Yokelson, R. J., Karl, T., Artaxo, P., Blake, D. R., Christian, T. J., Griffith, D. W. T., Guenther, A., and Hao, W. M.:
1270 The Tropical Forest and Fire Emissions Experiment: overview and airborne fire emission factor measurements,
1271 Atmos. Chem. Phys., 7, 5175–5196, doi:10.5194/acp-7-5175-2007, 2007.

1272 Yokelson, R. J., Christian, T. J., Karl, T. G., and Guenther, A.: The tropical forest and fire emissions experiment:
1273 laboratory fire measurements and synthesis of campaign data, Atmos. Chem. Phys., 8, 3509–3527, doi:10.5194/acp-
1274 8-3509-2008, 2008.

1275 Yokelson, R. J., Crounse, J. D., DeCarlo, P. F., Karl, T., Urbanski, S., Atlas, E., Campos, T., Shinozuka, Y.,
1276 Kapustin, V., Clarke, A. D., Weinheimer, A., Knapp, D. J., Montzka, D. D., Holloway, J., Weibring, P., Flocke, F.,
1277 Zheng, W., Toohey, D., Wennberg, P. O., Wiedinmyer, C., Mauldin, L., Fried, A., Richter, D., Walega, J., Jimenez,
1278 J. L., Adachi, K., Buseck, P. R., Hall, S. R., and Shetter, R.: Emissions from biomass burning in the Yucatan,
1279 Atmos. Chem. Phys., 9, 5785–5812, doi:10.5194/acp-9-5785-2009, 2009.

1280 Yokelson, R. J., Burling, I. R., Urbanski, S. P., Atlas, E. L., Adachi, K., Buseck, P. R., Wiedinmyer, C., Akagi, S.
1281 K., Toohey, D. W., and Wold, C. E.: Trace gas and particle emissions from open biomass burning in Mexico,
1282 Atmos. Chem. Phys. 11, 6787-6808, doi:10.5194/acpd-11-6787-2011, 2011.

1283 Yokelson, R. J., Burling, I. R., Gilman, J. B., Warneke, C., Stockwell, C. E., de Gouw, J., Akagi, S. K., Urbanski, S.
1284 P., Veres, P., Roberts, J. M., Kuster, W. C., Reardon, J., Griffith, D. W. T., Johnson, T. J., Hosseini, S., Miller, J.W.,
1285 Cocker III, D. R., Jung, H., and Weise, D. R.: Coupling field and laboratory measurements to estimate the emission
1286 factors of identified and unidentified trace gases for prescribed fires, Atmos. Chem. Phys., 13, 89–116,
1287 doi:10.5194/acp-13-89-2013, 2013a.

1288 Yokelson, R. J., Andreae, M. O., and Akagi, S. M.: Pitfalls with the use of enhancement ratios or normalized excess
1289 mixing ratios measured in plumes to characterize pollution sources and aging, Atmos. Meas. Tech., 6, 2155-2158,
1290 doi:10.5194/amt-6-2155-2013, 2013b.

1291 Zhang, J., Smith, K. R., Ma, Y., Ye, S., Qi, W., Liu, P., Khalil, M. A. K., Rasmussen, R. A., and Thorneloe, S.A.:
1292 Greenhouse Gases and other airborne pollutants from household stoves in China: a database for emission factors,
1293 Atmos. Environ., 34, 4537–49, 2000.

**Figure 1.** Excess mixing ratios of CO and $CO_2$ versus time for a (a) typical peat "stack" burn, (b) open cookstove "stack" burn (feeding fire), (c) grass "stack" burn, and (d) "room" burn.

**Figure 2.** Excess mixing ratios of 19 trace gases versus time for a complete sawgrass "stack" burn as measured by OP-FTIR.

**Figure 3.** Excess mixing ratios of sticky and non-sticky gases normalized by their maximum mixing ratio (shown in legend) to have a maximum value of one during a "room" burn of organic hay. The stable non-sticky species shown are CO and $CH_4$ while the stickier species include HCl, $NH_3$, glycolaldehyde, $CH_3COOH$, and HCOOH: the latter show a faster rate of decay than the stable species CO and $CH_4$.

**Figure 4.** Emission factors (g $kg^{-1}$) of select smoldering species as a function of MCE for FLAME-4 burns of African savanna fuels. Also shown are laboratory data of Christian et al. (2003), ground-based data of Wooster et al. (2011), and airborne data of Yokelson et al. (2003a). The linear fit based on all data is shown.

**Figure 5.** Comparison of EF versus MCE between FLAME-4 laboratory African grass fires (green) and airborne field measurements of African savanna fires (blue) for specified hydrocarbons, selected nitrogen containing species, and specified oxygenated species. Lines indicate linear regression of lab-based (green solid line) and airborne (blue dashed line) measurements.

**Figure 6.** The ratio of our Kalimantan peat fire EF to the EF from the single Sumatran peat fire of Christian et al. (2003). The upper and lower bounds of the bars represent ratios based on the range of our data, while the lines inside the bars represent the FLAME-4 study-average EF.

**Figure 7.** Emission factors (g $kg^{-1}$) for all nitrogen-containing species measured in current Kalimantan and past Sumatran laboratory peat fires (Christian et al., 2003). The Kalimantan peat room burn includes $NH_3$, a sticky species, thus the value should be considered a lower limit estimate.

**Figure 8.** Comparison of FLAME-4 3-stone, Envirofit G-3300 Rocket, and Philips HD4012 cookstove EF to EF reported during performance testing by Jetter et al. (2012). The Ezy stove was not tested by Jetter et al. (2012). Each circle represents the FLAME-4 fire average EF of all fuel types measured with all components starting at ambient temperatures compared to the Jetter et al (2012) data collected under regulated operating conditions.

**Figure 9**. Excess mixing ratio profiles of CO and $CO_2$ for both a traditional 3-stone cooking fire (104) and a more advanced "rocket" design stove (115) showing cleaner combustion and shorter time to reach a steady-state in the stove. The profiles of MCE versus time are included for both stove types.

**Figure 10.** Open cooking fire fire-averaged emission factors of $CH_4$ as a function of MCE for current and past laboratory and field measurements together with the recommended global averages. Error bars indicate the one standard deviation of EF for each study where available.

**Figure 11.** Emission factors of $NH_3$ as a function of MCE for "feed" crop residue fuels (triangles), "food" crop residue fuels (circles), and older millet samples (squares). Also shown are the lines of best fit from "food" fuels (green) and "feed" fuels (blue).

**Figure 12.** Glycolaldehyde EF as a function of MCE shown for current FLAME-4 CR, all remaining FLAME-4 fuels, a series of airborne measurements from US field campaigns, and laboratory rice straw measurements with error bars representing one standard deviation of EF where available.

**Figure 13**. Excess mixing ratio profiles of CO and $CO_2$ for the FLAME-4 plastic bag burn characterized by a large long-lived ratio of $\Delta CO_2/\Delta CO$ corresponding to strong flaming combustion.

1333 Table 1 Summary of fuels burned and fuel elemental analysis (see Sect. 2.2 for fuel descriptions).

| Fuel | Stack Exp. | Room Exp. | Environmental Chamber Exp. | Fuel Type | Sampling Location (s) | C-Content (%) | N-Content (%) | Cl / S-Content (%) | Ash |
|---|---|---|---|---|---|---|---|---|---|
| African grass (tall) | 11 | 1 | 0 | Savanna/Sourveld/Tall grass | Kruger National Park, R.S.A. | 43.56 - 43.82 | 0.21 - 0.32 | bdl / 0.063 | 4.7 |
| African grass (short) | 8 | 0 | 0 | Savanna/Sweetveld/Short grass | Kruger National Park, R.S.A. | 43.56 - 44.56 | 0.47 - 0.70 | 0.19 / 0.21 | 3.5 - 5.4 |
| Giant Cutgrass | 5 | 3 | 2 | Marsh | Jasper Co., SC | 44.84 | 2.03 | 0.34 / 0.21 | 2.3 |
| Sawgrass | 12 | 1 | 0 | Marsh | Jasper Co., SC | 45.83 | 0.93 | 0.77 / 0.16 | 3.5 |
| Wiregrass | 7 | 2 | 1 | Pine forest understory | Chesterfield Co., SC | 46.70 | 0.61 | bdl | - |
| Peat (CAN) | 3 | 0 | 0 | Boreal Peat | Ontario & Alberta, CAN | 44.05 - 46.74 | 0.93 - 1.22 | nm | 7.6 - 9.2 |
| Peat (NC) | 2 | 1 | 0 | Temperate Peat | Green Swamp & Alligator River NWR, NC | 25.79 - 51.12 | 0.63 - 1.26 | nm / 0.12 | 14.7 - 58.4 |
| Peat (IN) | 2 | 1 | 1 | Indonesian Peat | South Kalimantan | 53.83 – 59.71 | 2.03 - 2.50 | nm / 0.12 | 1.4 – 3.8 |
| Organic Alfalfa | 3 | 0 | 0 | Crop residue | Fort Collins, CO | 42.28 | 2.91 | nm / 0.29 | 4.4 |
| Organic Hay | 6 | 2 | 1 | Crop residue | Fort Collins, CO | 41.39 | 1.99 | 1.13 / 0.22 | 7.7 |
| Organic Wheat Straw | 6 | 2 | 0 | Crop residue | Fort Collins, CO | 43.32 | 0.40 | 0.32 / 0.085 | 3.7 |
| Conventional Wheat Straw | 2 | 0 | 0 | Crop residue | Maryland | 43.53 | 0.39 | 2.57 | 3.4 |
| Conventional Wheat Straw | 2 | 1 | 0 | Crop residue | Walla Walla Co., WA | 40.20 | 0.69 | bdl | 10.4 |
| Sugar Cane | 2 | 1 | 0 | Crop residue | Thibodaux, LA | 41.33 | 0.76 | 0.4 | 9.1 |
| Rice Straw | 7 | 4 | 1 | Crop residue | CA, China, Malaysia, Taiwan | 37.85 - 42.07 | 0.88 - 1.30 | 0.61 / 0.14-0.21 | 7.7 - 12.2 |
| Millet | 3 | 0 | 0 | Crop residue & Cookstove fuel | Ghana | 43.58 | 0.08 | nm | 7.4 |
| Red Oak | 5 | 0 | 0 | Cookstove fuel | Commercial lumberyard | 46.12 | 0.09 | nm / 0.009 | 5.9 |
| Douglas Fir | 3 | 0 | 0 | Cookstove fuel | Commercial lumberyard | 46.70 | bdl | nm | - |
| Okote | 2 | 0 | 2 | Cookstove fuel | Honduras via Commercial lumberyard | 45.09 | bdl | nm / 0.011 | 8.5 |
| Trash | 2 | 0 | 0 | Trash or waste | Missoula, MT | 50.29 - 50.83[a] | nm | nm | - |
| Shredded Tires | 2 | 0 | 0 | Trash or waste | Iowa City, IA | 81.98[b] | 0.57 | nm /1.56[b] | - |
| Plastic Bags | 1 | 0 | 0 | Trash or waste | Missoula, MT | 74.50[c] | nm | nm | - |
| Juniper | 2 | 0 | 0 | Temperate Forest | Outskirts Missoula, MT | 50.73 | 1.17 | nm | 4.0 |
| Ponderosa Pine | 11 | 5 | 10 | Temperate Forest | Outskirts Missoula, MT | 51.11 | 1.09 | nm | 1.5 |
| Black Spruce | 5 | 7 | 9 | Boreal Forest | South of Fairbanks, AK | 50.50 | 0.66 | nm / 0.054 | 3.8 |
| Chamise | 7 | 1 | 0 | Chaparral | San Jacinto Mtns, CA | 50.27 | 1.00 | nm / 0.060 | - |
| Manzanita | 3 | 1 | 0 | Chaparral | San Jacinto Mtns, CA | 49.89 | 0.73 | nm / 0.049 | - |
| **Total** | **124** | **33** | **27** | | | | | | |

Note: "nm" indicates not measure, "bdl" indicates below the detection limit

[a] estimated using approach described in Christian et al. [2010] and Sect. 3.5

[b] estimated from Table 1 in Martinez et al. [2013]

[c] estimated using USEPA (2010)

Table 2. Summary of the comparison of emission factors and emission ratios (to CO) measured in the lab and field for savanna fuels and projected emission factors for US grasses calculated at the savanna grass field average MCE. Values in parentheses are one standard deviation.

| Species | African Savanna grass | | | | | | US grasses |
|---|---|---|---|---|---|---|---|
| | Field Yokelson et al. [2003a] (EF) | Lab FLAME predict at field avg MCE (EF) | Lab EF predict / Field EF avg | Field Yokelson et al. [2003a] (ER) | Lab FLAME-4 (ER) | Field ER avg / Lab ER avg | Lab FLAME predict at field avg MCE (EF) |
| MCE | 0.938 | 0.938 | - | 0.938 | 0.978 | - | 0.938 |
| Carbon Dioxide ($CO_2$) | 1703 | - | - | - | - | - | - |
| Carbon Monoxide (CO) | 71.5 | - | - | 1 | 1 | 1 | - |
| Methane ($CH_4$) | 2.19 | 2.29 | 1.04 | 0.053(0.012) | 0.029(0.012) | 1.83 | 2.16 |
| Acetylene ($C_2H_2$) | 0.260 | 0.251 | 0.967 | 0.004(0.001) | 0.003(0.001) | 1.45 | 0.448 |
| Ethylene ($C_2H_4$) | 1.19 | 1.15 | 0.969 | 0.017(0.003) | 0.008(0.004) | 2.01 | 0.918 |
| Methanol ($CH_3OH$) | 1.17 | 1.21 | 1.03 | 0.014(0.003) | 0.005(0.004) | 2.77 | 0.339 |
| Formaldehyde (HCHO) | 1.06 | 2.56 | 2.41 | 0.015(0.004) | 0.016(0.008) | 0.915 | 0.529 |
| Acetic Acid ($CH_3COOH$) | 2.42 | 4.05 | 1.68 | 0.016(0.002) | 0.013(0.007) | 1.26 | 0.873 |
| Formic Acid (HCOOH) | 0.270 | 0.336 | 1.25 | 0.003(0.002) | 0.002(0.001) | 1.55 | 0.064 |
| Ammonia ($NH_3$) | 0.280 | 0.691 | 2.47 | 0.007(0.004) | 0.006(0.004) | 1.19 | 0.709 |
| Hydrogen Cyanide (HCN) | 0.530 | 0.301 | 0.569 | 0.009(0.003) | 0.005(0.001) | 1.70 | 0.561 |
| Nitrogen Oxides ($NO_x$ as NO) | 3.37 | 3.20 | 0.950 | - | - | - | 2.16 |
| Average | | | 1.33(0.65) | | | 1.63(0.54) | |
| Hydrocarbon avg. | | | 0.994(0.044) | | | 1.76(0.28) | |
| N-species avg. | | | 1.33(1.00) | | | 1.45(0.36) | |
| OVOC avg. | | | 1.59(0.61) | | | 1.62(0.80) | |

Table 3. Comparison of emission factors (g $kg^{-1}$) for three laboratory peat studies including Yokelson et al. (1997), Christian et al. (2003), and FLAME-4. The average and one standard deviation are shown for each peat type during the study and an overall regional EF is shown for extratropical and Indonesian peat. Values in parentheses are one standard deviation.

| Species | Peat Emissions | | | | | | |
|---|---|---|---|---|---|---|---|
| | Peat Canadian | Peat NC | Peat AK & MN[a] | Overall Extratropical Peat | Kalimantan peat | Sumatran peat[b] | Overall Indonesian Peat |
| MCE | 0.805(0.009) | 0.726(0.067) | 0.809(0.327) | 0.766(0.061) | 0.816(0.065) | 0.838 | 0.821(0.054) |
| Carbon Dioxide ($CO_2$) | 1274(19) | 1066(287) | 1395(52) | 1190(231) | 1637(204) | 1703 | 1653(170) |
| Carbon Monoxide (CO) | 197(9) | 276(139) | 209(68) | 238(97) | 233(72) | 210 | 227(60) |
| Methane ($CH_4$) | 6.25(2.17) | 10.9(5.3) | 6.85(5.66) | 8.67(4.27) | 12.8(6.6) | 20.8 | 14.8(6.7) |
| Acetylene ($C_2H_2$) | 0.10(0.00) | 0.16(0.08) | 0.10(0.00) | 0.13(0.06) | 0.18(0.05) | 0.059 | 0.15(0.07) |
| Ethylene ($C_2H_4$) | 0.81(0.29) | 1.27(0.77) | 1.37(0.51) | 1.13(0.56) | 1.39(0.62) | 2.57 | 1.68(0.78) |
| Propylene ($C_3H_6$) | 0.50(0.00) | 1.17(0.63) | 2.79(0.44) | 1.36(0.96) | 1.49(0.63) | 3.05 | 1.88(0.94) |
| Methanol ($CH_3OH$) | 0.75(0.35) | 2.83(2.87) | 4.04(3.43) | 2.34(2.25) | 3.24(1.39) | 8.69 | 4.60(2.95) |
| Formaldehyde (HCHO) | 1.43(0.37) | 1.41(1.16) | 1.99(2.67) | 1.51(0.79) | 1.25(0.79) | 1.40 | 1.29(0.65) |
| Furan ($C_4H_4O$) | 0.88(0.04) | 1.78(1.84) | - | 1.42(1.39) | 0.89(0.27) | 1.91 | 1.15(0.56) |
| Nitrous Acid (HONO) | 0.18(0.00) | 0.48(0.50) | - | 0.38(0.39) | 0.10 | - | 0.10 |
| Nitric Oxide (NO) | - | 0.51(0.12) | - | 0.51(0.12) | 1.85(0.56) | 1.00 | 1.57(0.63) |
| Nitrogen Dioxide ($NO_2$) | - | 2.31(1.46) | - | 2.31(1.46) | 2.36(0.03) | - | 2.36(0.03) |
| Hydrogen Cyanide (HCN) | 1.77(0.55) | 4.45(3.02) | 5.09(5.64) | 3.66(2.43) | 3.30(0.79) | 8.11 | 4.50(2.49) |
| Acetic Acid ($CH_3COOH$) | 1.86(1.35) | 8.46(8.46) | 7.29(4.89) | 5.59(5.49) | 7.65(3.65) | 8.97 | 8.09(2.69) |
| Formic Acid (HCOOH) | 0.40(0.06) | 0.44(0.34) | 0.89(1.50) | 0.51(0.27) | 0.55(0.05) | 0.38 | 0.49(0.11) |
| Glycolaldehyde ($C_2H_4O_2$) | - | - | 1.66(2.64) | 1.66 | - | - | - |
| Hydrogen Chloride (HCl) | - | 7.68E-03 | - | 7.68E-03 | - | - | - |
| Ammonia ($NH_3$) | 2.21(0.24) | 1.87(0.37) | 8.76(13.76) | 3.38(3.02) | 1.39(0.97) | 19.9 | 7.57(10.72) |

[a]Source is *Yokelson et al*. [1997]

[b]Source is *Christian et al.* [2003]

Table 4. Fire-average emission factors (g $kg^{-1}$) for cookstoves. The average emission ratios to CO for smoldering compounds are also shown for 3-stone traditional cooking fires.

| Species | Traditional and Advanced Cooking stoves | | | | | | | | | |
|---|---|---|---|---|---|---|---|---|---|---|
| | 3 stone (EF) | | | | Envirofit G3300 Rocket (EF) | | | Ezy stove (EF) | | Philips HD4012(EF) |
| | Doug Fir | Okote | Red Oak | ER avg (stdev) | Doug Fir | Okote | Red Oak | Millet | Red Oak | Doug Fir |
| MCE | 0.963 | 0.968 | 0.972 | 0.968(0.004) | 0.974 | 0.966 | 0.985 | 0.950 | 0.985 | 0.984 |
| Carbon Dioxide ($CO_2$) | 1640 | 1589 | 1628 | - | 1662 | 1586 | 1661 | 1503 | 1656 | 1682 |
| Carbon Monoxide (CO) | 39.8 | 33.5 | 30.2 | - | 28.1 | 35.8 | 15.9 | 49.9 | 16.3 | 17.3 |
| Methane ($CH_4$) | 1.27 | 1.37 | 1.29 | 0.067(0.010) | 0.90 | 1.32 | 0.23 | 2.64 | 0.41 | 0.37 |
| Acetylene ($C_2H_2$) | 0.41 | 1.07 | 0.41 | 0.020(0.013) | 0.055 | 1.26 | 0.052 | 0.42 | 0.23 | 0.16 |
| Ethylene ($C_2H_4$) | 0.39 | 1.03 | 0.37 | 0.018(0.012) | 0.11 | 0.83 | 0.063 | 0.84 | 0.21 | 0.16 |
| Propylene ($C_3H_6$) | bdl | 0.11 | 0.058 | 0.002(0.001) | bdl | bdl | bdl | bdl | 0.012 | 0.006 |
| Water ($H_2O$) | 0.10 | 0.14 | 0.15 | 0.006(0.002) | 0.15 | 0.14 | 0.14 | 0.089 | 0.19 | 0.23 |
| Methanol ($CH_3OH$) | 0.70 | 0.057 | 0.90 | 0.014(0.012) | 0.56 | 0.066 | 0.43 | 0.77 | 0.81 | 0.087 |
| Formaldehyde (HCHO) | 0.63 | 0.24 | 0.50 | 0.012(0.005) | 0.51 | 0.25 | 0.21 | 0.82 | 0.40 | 0.21 |
| Formic Acid (HCOOH) | 0.14 | 0.037 | 0.32 | 0.003(0.003) | 0.17 | 0.038 | 0.15 | 0.13 | 0.24 | 0.050 |
| Acetic Acid ($CH_3COOH$) | 0.63 | bdl | 4.16 | 0.036(0.040) | 0.72 | bdl | 1.74 | 1.98 | 2.99 | 0.076 |
| Furan ($C_4H_4O$) | 0.087 | bdl | 0.087 | 0.001(0.000) | bdl | bdl | bdl | bdl | 0.016 | bdl |
| Glycolaldehyde ($C_2H_4O_2$) | 0.094 | bdl | 0.15 | 0.002(0.001) | 0.18 | bdl | bdl | bdl | 0.11 | 0.26 |
| Nitric Oxide (NO) | 0.34 | 0.24 | 0.42 | - | 0.48 | 0.29 | 0.65 | 1.03 | 0.57 | 0.61 |
| Nitrogen Dioxide ($NO_2$) | 1.04 | 0.94 | 1.49 | - | 1.14 | bdl | 0.98 | bdl | 1.57 | 1.66 |
| Hydrogen Cyanide (HCN) | bdl | 0.061 | 0.059 | 0.002(0.000) | bdl | 0.043 | bdl | bdl | bdl | bdl |
| Nitrous Acid (HONO) | 0.18 | 0.51 | 0.22 | 0.005(0.003) | bdl | 0.66 | bdl | bdl | bdl | bdl |
| Ammonia ($NH_3$) | 0.019 | bdl | 0.023 | 0.001(0.000) | 0.021 | 7.09E-04 | 0.022 | 0.23 | 0.018 | 0.011 |
| Hydrogen chloride (HCl) | bdl | bdl | bdl | - | bdl | bdl | bdl | bdl | bdl | bdl |
| Sulfur Dioxide ($SO_2$) | bdl | 0.52 | bdl | - | bdl | bdl | bdl | bdl | bdl | bdl |

Note: "bdl" indicates mixing ratio was below detection limit

Table 5. Summary of the comparison of emission factors and emission ratios (to CO) measured in the lab and field for crop residue fuels. Values in parentheses are one standard deviation.

| Species | Crop Residue | | | | | |
|---|---|---|---|---|---|---|
| | Field Akagi et al. [2011][a] (EF) | Lab FLAME-4[b] predict at field avg MCE (EF) | Lab EF predict / Field EF avg | Field Akagi et al. [2011] (ER) | Lab FLAME-4 (ER) | Field ER avg / Lab ER avg |
| MCE | 0.925 | 0.925 | - | 0.925 | 0.946 | - |
| Carbon Dioxide ($CO_2$) | 1664 | - | - | - | - | - |
| Carbon Monoxide (CO) | 85.6 | - | - | - | - | - |
| Methane ($CH_4$) | 5.01 | 3.66 | 0.730 | 0.102(0.051) | 0.072(0.018) | 1.42 |
| Acetylene ($C_2H_2$) | 0.230 | 0.346 | 1.50 | 0.003(0.001) | 0.005(0.003) | 0.542 |
| Ethylene ($C_2H_4$) | 1.16 | 1.40 | 1.21 | 0.014(0.007) | 0.017(0.006) | 0.787 |
| Propylene ($C_3H_6$) | 0.496 | 0.605 | 1.22 | 0.004(0.002) | 0.004(0.002) | 0.920 |
| Methanol ($CH_3OH$) | 2.67 | 1.97 | 0.738 | 0.027(0.014) | 0.017(0.008) | 1.60 |
| Formaldehyde (HCHO) | 1.85 | 2.02 | 1.10 | 0.020(0.010) | 0.024(0.011) | 0.840 |
| Acetic Acid ($CH_3COOH$) | 4.52 | 4.07 | 0.901 | 0.025(0.012) | 0.019(0.013) | 1.32 |
| Formic Acid (HCOOH) | 1.00 | 0.669 | 0.669 | 0.007(0.004) | 0.003(0.003) | 2.36 |
| Nitric Oxide (NO) | 2.06 | 1.49 | 0.721 | - | - | - |
| Nitrogen Dioxide ($NO_2$) | 3.48 | 1.71 | 0.491 | - | - | - |
| Nitrogen Oxides ($NO_x$ as NO) | 3.64 | 2.08 | 0.572 | - | - | - |
| Ammonia ($NH_3$) | 1.76 | 1.15 | 0.654 | 0.034(0.017) | 0.016(0.011) | 2.07 |
| Hydrogen Cyanide (HCN) | 0.160 | 0.399 | 2.49 | 0.002(0.001) | 0.005(0.002) | 0.421 |
| Absolute average | | | 1.00(0.54) | | | 1.23(0.64) |
| Hydrocarbon avg. | | | 1.17(0.32) | | | 0.918(0.370) |
| N-species avg. | | | 0.986(0.847) | | | 1.24(1.16) |
| OVOC avg. | | | 0.851(0.191) | | | 1.53(0.64) |

[a] Supplementary Table 13 in Akagi et al. [2011]

[b] Fuels grouped as food sources as detailed in Sect. 3.4

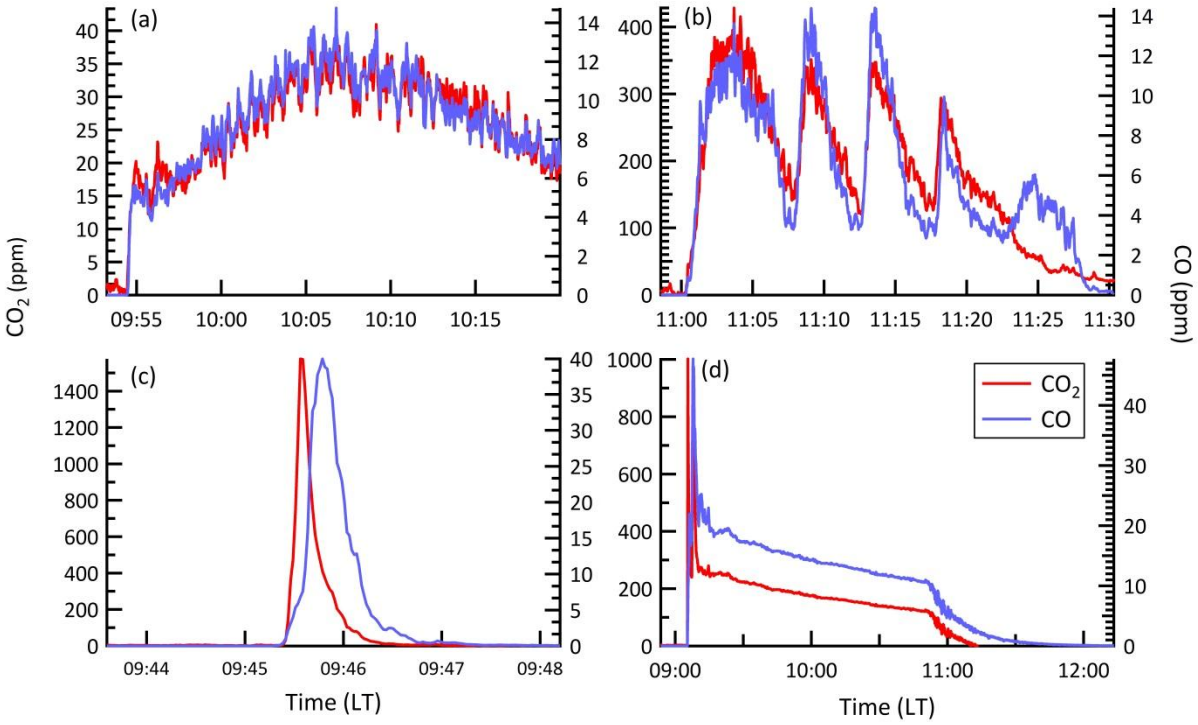


Figure 1. Excess mixing ratios of CO and $CO_2$ versus time for a (a) typical peat "stack" burn, (b) open cookstove "stack" burn (feeding fire), (c) grass "stack" burn, and (d) "room" burn.

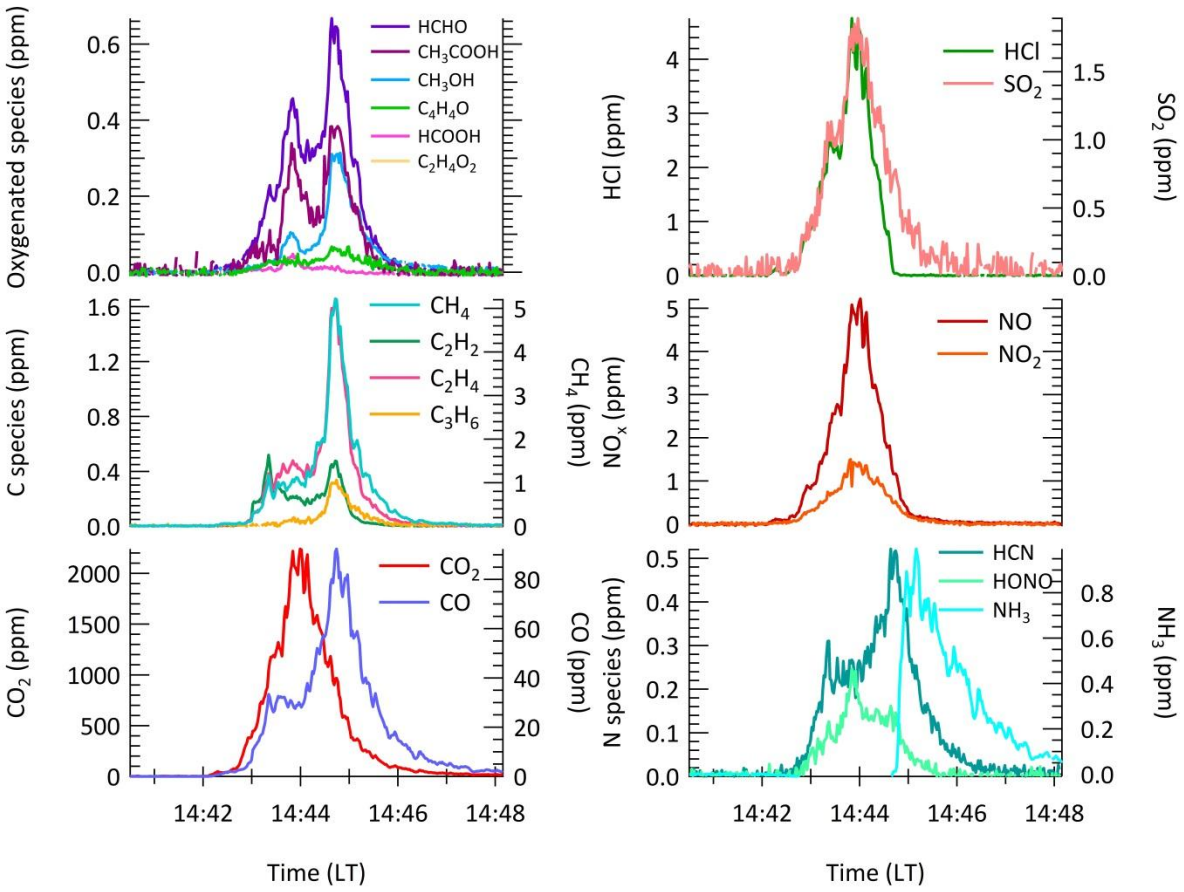


Figure 2. Excess mixing ratios of 19 trace gases versus time for a complete sawgrass "stack" burn as measured by OP-FTIR.

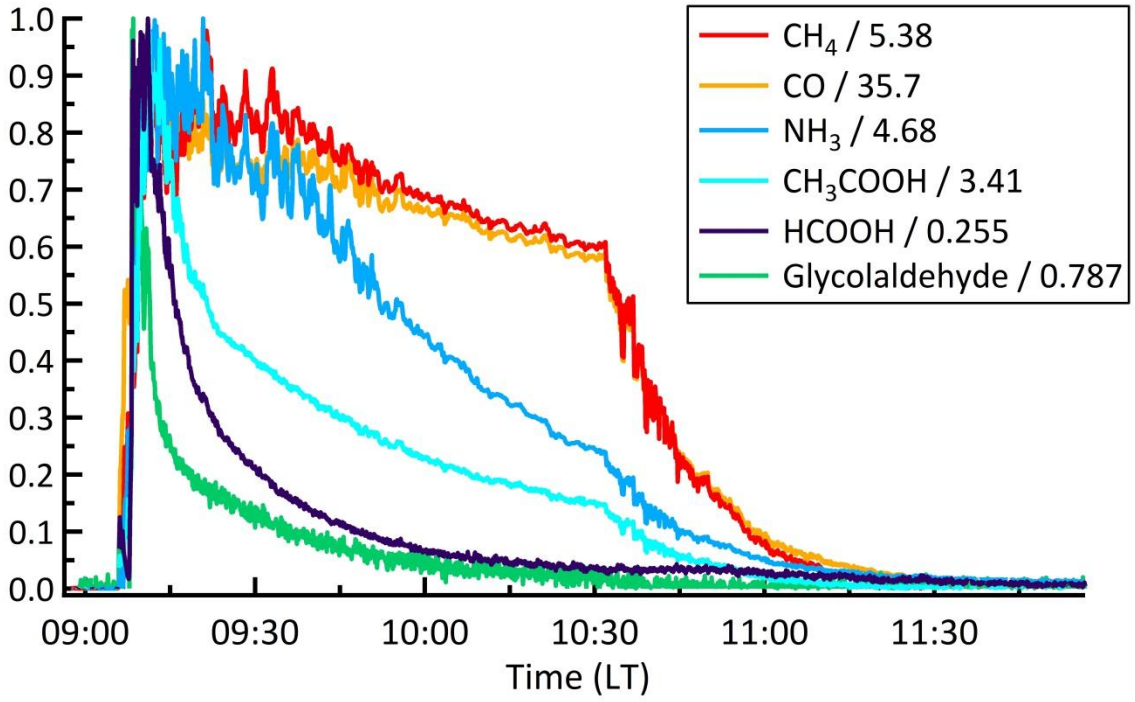


Figure 3. Excess mixing ratios of sticky and non-sticky gases normalized by their maximum mixing ratio (shown in legend) to have a maximum value of one during a "room" burn of organic hay. The stable non-sticky species shown are CO and $CH_4$ while the stickier species include HCl, $NH_3$, glycolaldehyde, $CH_3COOH$, and HCOOH: the latter show a faster rate of decay than the stable species CO and $CH_4$.

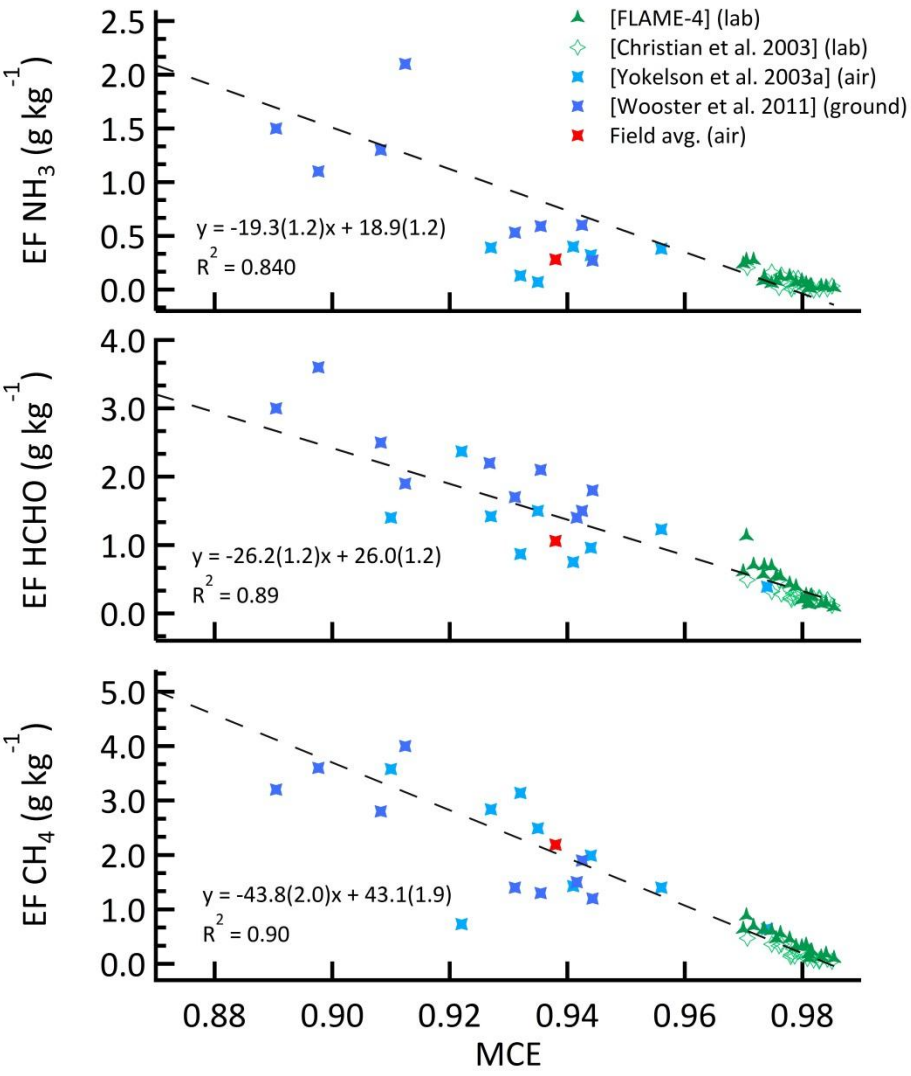


Figure 4. Emission factors (g $kg^{-1}$) of select smoldering species as a function of MCE for FLAME-4 burns of African savanna fuels. Also shown are laboratory data of Christian et al. (2003), ground-based data of Wooster et al. (2011), and airborne data of Yokelson et al. (2003a). The linear fit based on all data is shown.

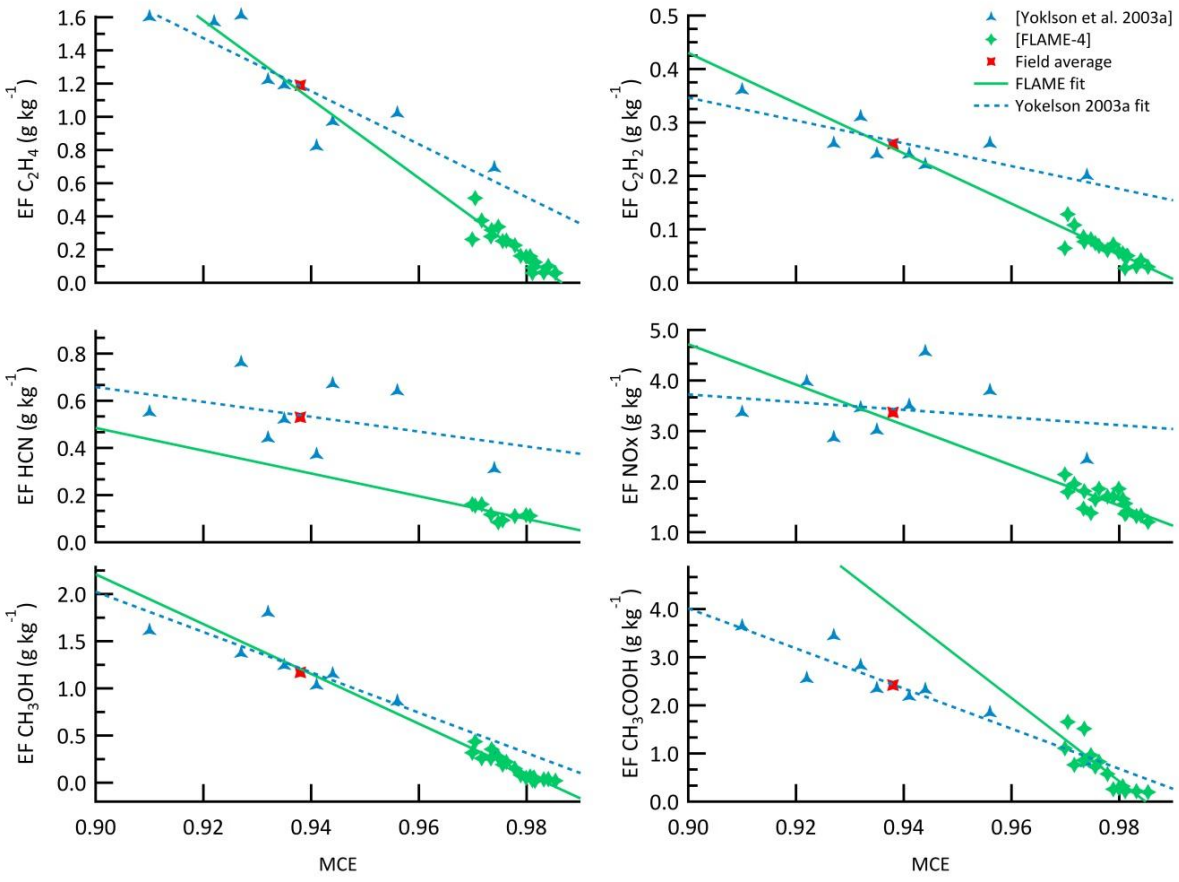


Figure 5. Comparison of EF versus MCE between FLAME-4 laboratory African grass fires (green) and airborne field measurements of African savanna fires (blue) for specified hydrocarbons, selected nitrogen containing species, and specified oxygenated species. Lines indicate linear regression of lab-based (green solid line) and airborne (blue dashed line) measurements.

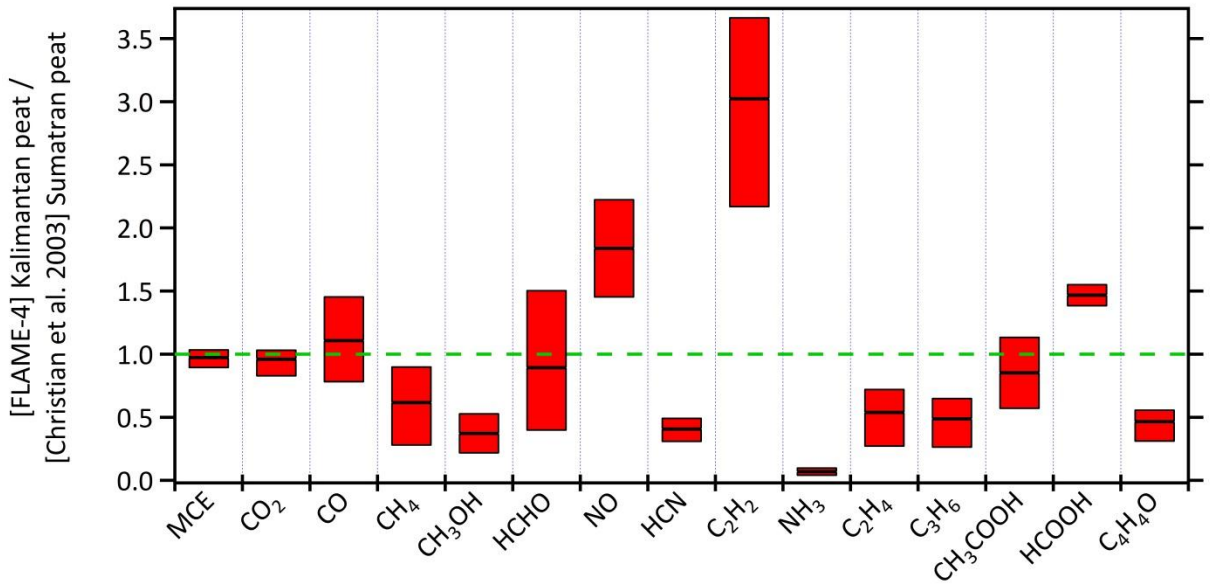


Figure 6. The ratio of our Kalimantan peat fire EF to the EF from the single Sumatran peat fire of Christian et al. (2003). The upper and lower bounds of the bars represent ratios based on the range of our data, while the lines inside the bars represent the FLAME-4 study-average EF.

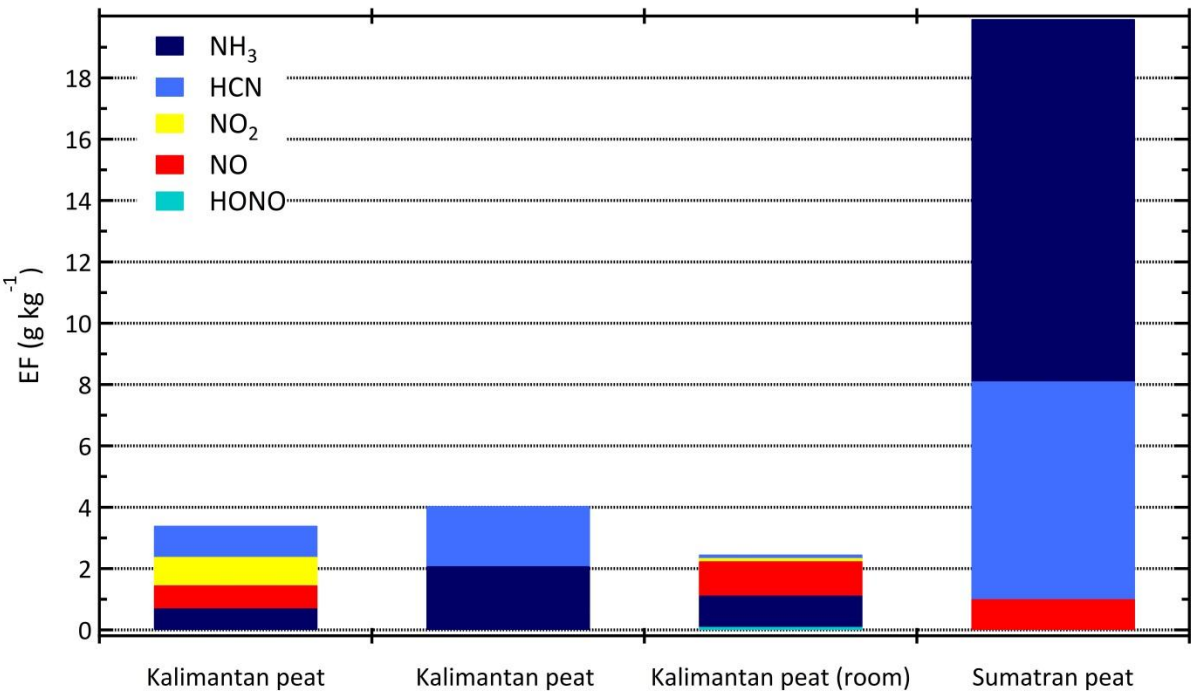


Figure 7. Emission factors (g $kg^{-1}$) for all nitrogen-containing species measured in current Kalimantan and past Sumatran laboratory peat fires (Christian et al., 2003). The Kalimantan peat room burn includes $NH_3$, a sticky species, thus the value should be considered a lower limit estimate.

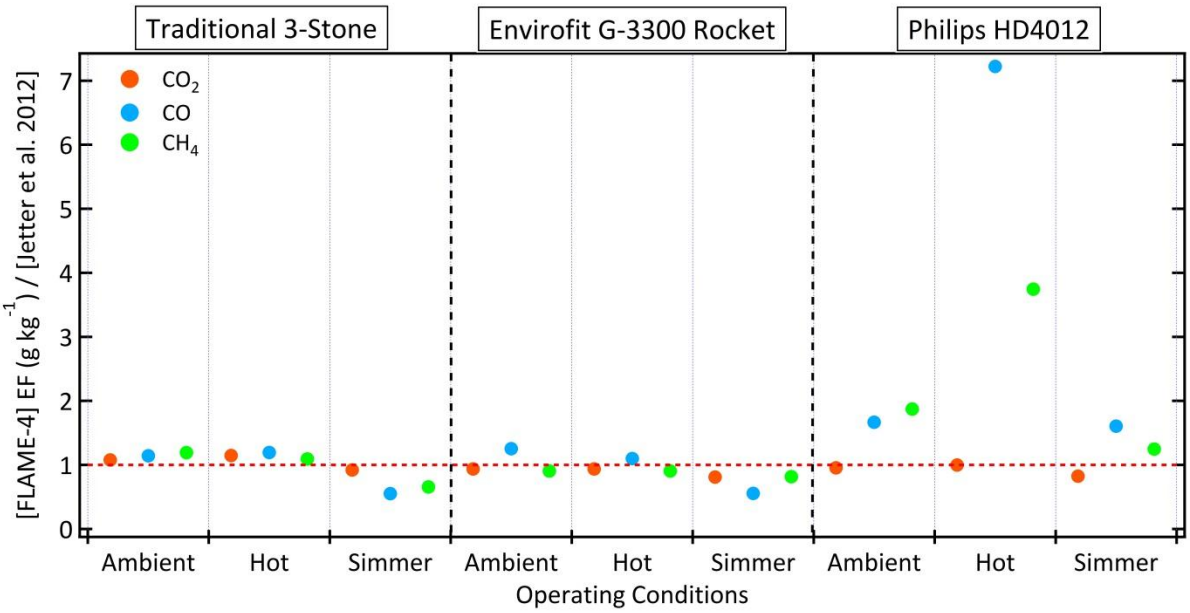


Figure. 8. Comparison of FLAME-4 3-stone, Envirofit G-3300 Rocket, and Philips HD4012 cookstove EF to EF reported during performance testing by Jetter et al. (2012). The Ezy stove was not tested by Jetter et al. (2012). Each circle represents the FLAME-4 fire average EF of all fuel types measured with all components starting at ambient temperatures compared to the Jetter et al (2012) data collected under regulated operating conditions.

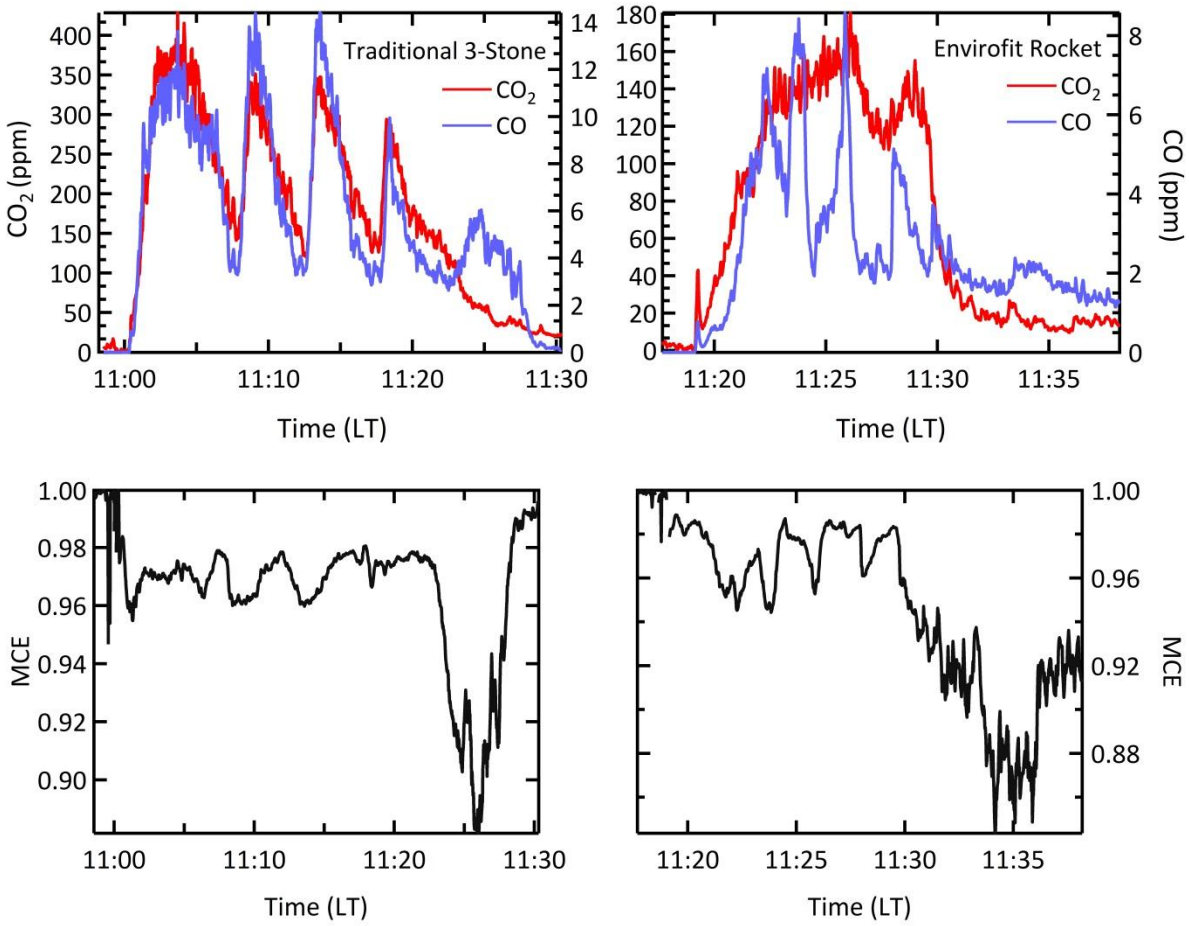


Figure 9. Excess mixing ratio profiles of CO and $CO_2$ for both a traditional 3-stone cooking fire (104) and a more advanced "rocket" design stove (115) showing cleaner combustion and shorter time to reach a steady-state in the stove. The profiles of MCE versus time are included for both stove types.

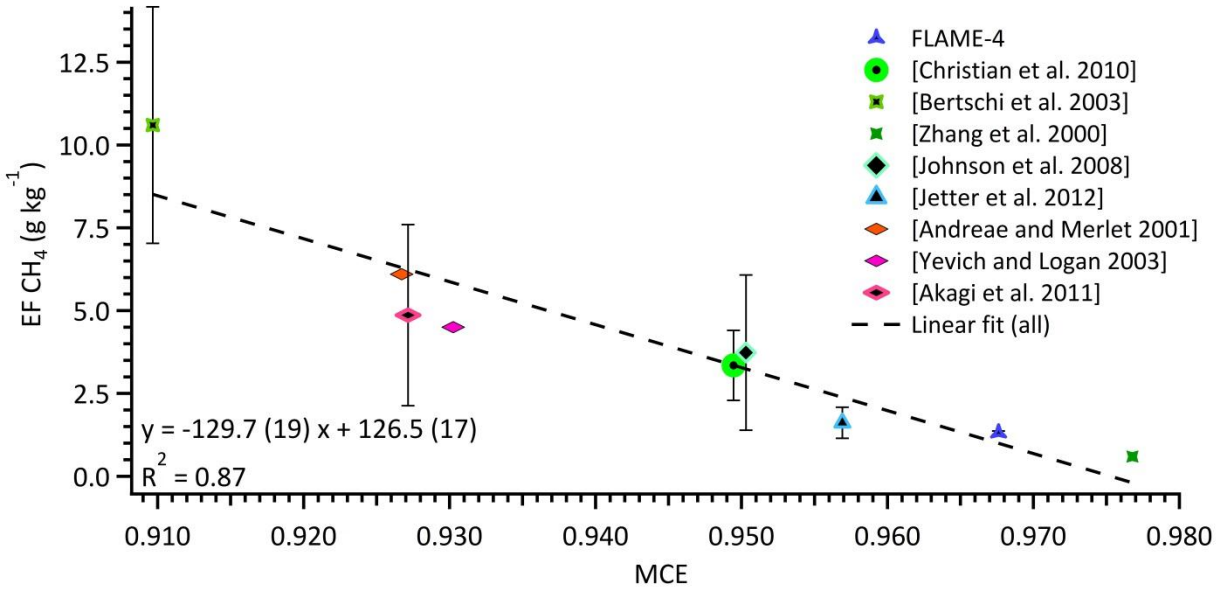


Figure 10. Open cooking fire fire-averaged emission factors of $CH_4$ as a function of MCE for current and past laboratory and field measurements together with the recommended global averages. Error bars indicate the one standard deviation of EF for each study where available.

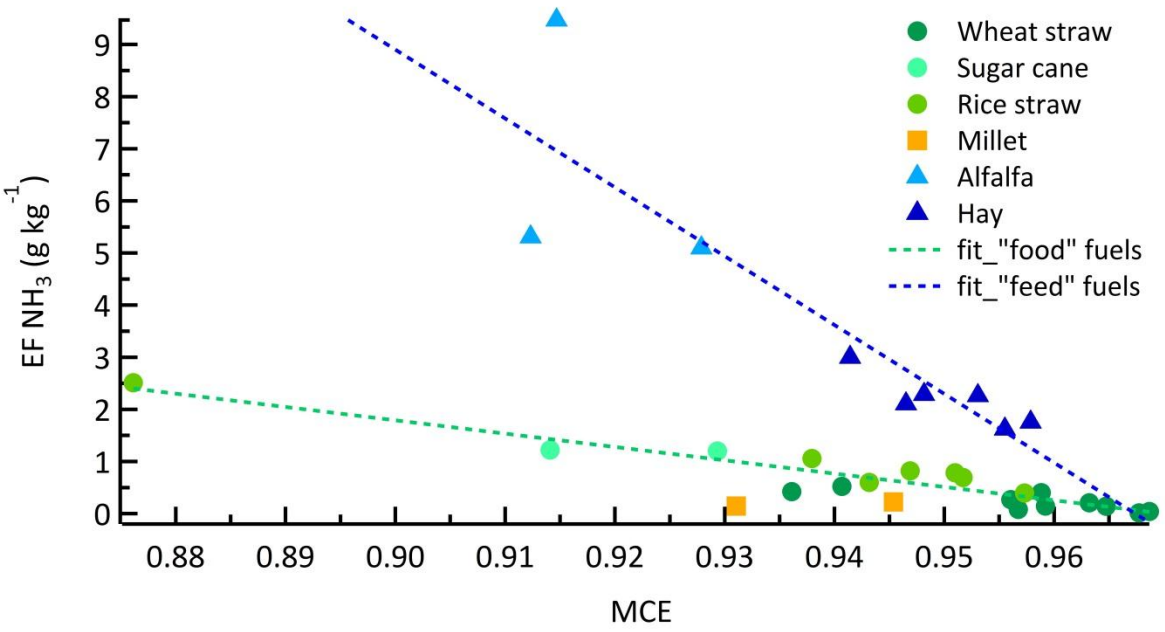


Figure 11. Emission factors of $NH_3$ as a function of MCE for "feed" crop residue fuels (triangles), "food" crop residue fuels (circles), and older millet samples (squares). Also shown are the lines of best fit from "food" fuels (green) and "feed" fuels (blue).

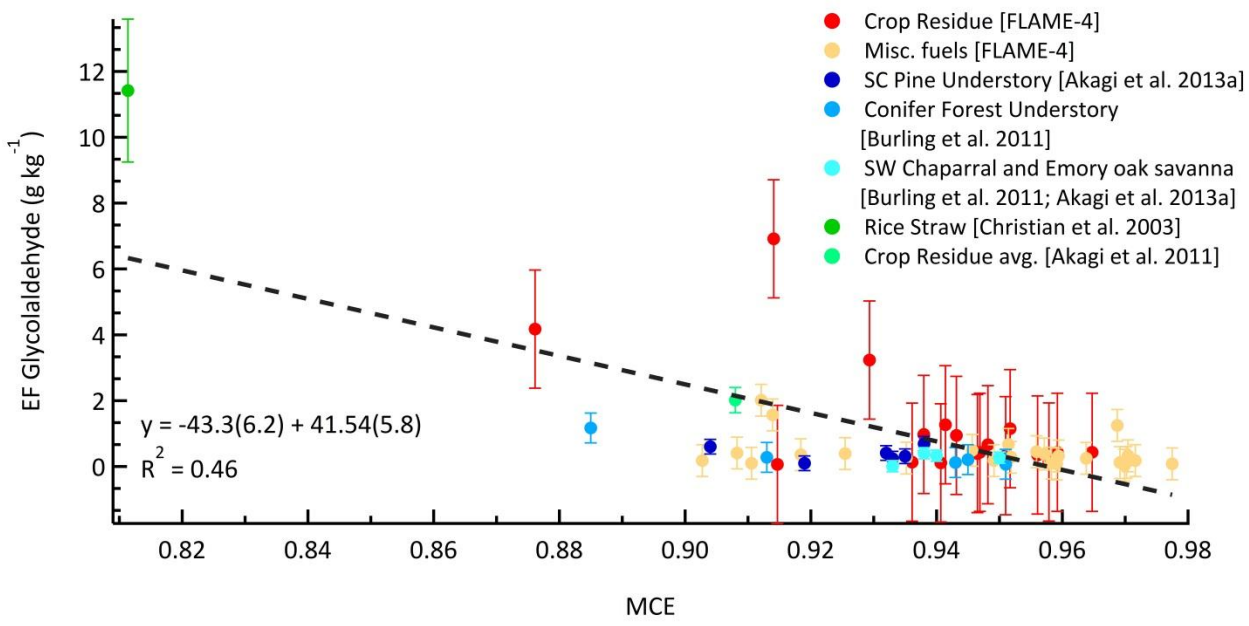


Figure 12. Glycolaldehyde EF as a function of MCE shown for current FLAME-4 CR, all remaining FLAME-4 fuels, a series of airborne measurements from US field campaigns, and laboratory rice straw measurements with error bars representing one standard deviation of EF where available.

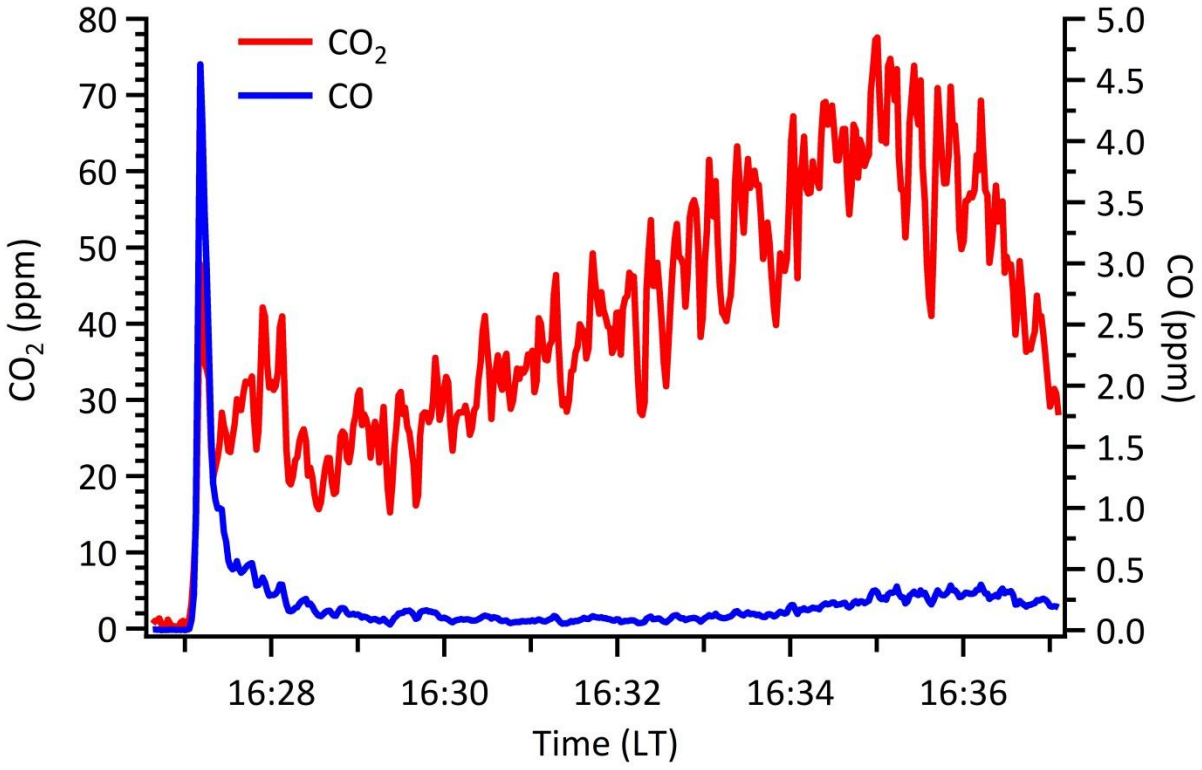


Figure 13. Excess mixing ratio profiles of CO and $CO_2$ for the FLAME-4 plastic bag burn characterized by a large long-lived ratio of $\Delta CO_2/\Delta CO$ corresponding to strong flaming combustion.